Supplementary Materials

A multichannel nanosensor for instantaneous readout of cancer drug mechanisms

Subinoy Rana,[1] Ngoc D. B. Le,[1,#] Rubul Mout,[1,#] Krishnendu Saha,[1] Gulen Yesilbag Tonga,[1] Robert E. S. Bain,[3] Oscar R. Miranda,[1] Caren M. Rotello[2] & Vincent M. Rotello[1]*

[1]Department of Chemistry, [2]Department of Psychology, University of Massachusetts Amherst, 710 N. Pleasant St., Amherst, MA 01003, USA. [3]Department of Materials, Imperial College London, South Kensington Campus, London SW7 2AZ, UK.

Table of Contents

Section 1: Synthesis of the Sensor Elements

1.1 Cloning and expression of fluorescent proteins. Genetic manipulations and bacterial culture were performed according to standard protocols. The gene encoding EBFP2 protein was PCR amplified from a pBad-EBFP2 plasmid[1] (Addgene, No. 14891) using primers 5′-ACGATGGAT CCATGGTGAG C-3′ (forward) and 5′-GTGACAAGCTTTTACTTGTACAG-3′ (reverse). The amplified product was cloned into pQE80 vector digested with *Bam*HI and *Hind*III restriction sites (downstream of 6xHis tag) to obtain the expression construct pQE80-6xHis-EBFP2.

To construct pQE80-6xHis-tdTomato plasmid, tdTomato gene was sub-cloned from pASTA3 (from Addgene[2,3]) plasmid into *Bam*HI and *Hind*III (downstream of 6xHis tag) restriction sites of pQE80 expression vector. pET21d-EGFP plasmid (Novagen[4]) containing 6xHis tag in the N-terminus was used for EGFP expression.

To produce recombinant proteins, *Escherichia coli* BL21(DE3) strain was transformed with the respective plasmids. Transformed colonies were picked up to grow small cultures in 50 mL 2xYT media at 37^0C for overnight. The following day, 15 mL of grown culture was inoculated into one liter 2xYT media and allowed to grow at 37^0C until optical density (OD) at 600 nm reaches ~0.6. At this point, the protein expression was induced by adding isopropyl-β-D-thiogalactopyranoside (IPTG; 1 mM final concentration) at 25^0C. After four hours of induction, the cells were harvested and the pellets were lysed using microfluidizer. His-tag fluorescent proteins were purified from the lysed supernatant using Co^{2+}-nitrilotriacetate columns (HisPur™ cobalt spin columns, Pierce, Thermo Scientific). The integrity and the expression of native protein were confirmed by 12% SDS-PAGE gel, absorbance, and fluorescence spectra.

1.2 Synthesis of BenzNP. The organic ligand and the NP core were synthesized following the previous report[5,6]. This section describes the full experimental details of all performed reactions for the syntheses of the ligand and the particle, as well as their standard characterizations (^{1}H NMR spectra and Supplementary Fig. 1 – 3).

1.2.1 General. All chemicals and solvents for syntheses were purchased from Fisher Scientific, except $HAuCl_4$ that was purchased from Strem Chemicals Inc., and used without further purification, unless otherwise stated. Yields refer to chromatographically and spectroscopically (^{1}H NMR) homogeneous material, unless otherwise stated. Reactions were monitored by thin-layer chromatography performed on 0.25 mm Sorbent Technologies aluminium backed silica gel plates (w/UV254), using ultraviolet radiation as the visualizing agent and one of the following as developing agents: an acidic solution of ceric ammonium molybdate and heat, or $KMnO_4$/heat.

1.2.2 NMR spectroscopy. NMR spectra were recorded on Bruker Avance 400 instrument and were calibrated using residual undeuterated solvent as an internal reference ($CHCl_3$ at 7.26 p.p.m. ^{1}H-NMR). The following abbreviations were used to explain NMR peak multiplicities: s, singlet; d, doublet; t, triplet; q, quartet; p, quintet (pentet); m, multiplet; br, broad (see the ^{1}H NMR spectra section).

1.2.3 Mass spectrometry. Matrix assisted laser desorption/ionization mass spectrometry (MALDI-MS) has been performed to characterize the surface ligand on the **BenzNP**. A saturated α-cyano-4-hydroxycinnamic acid (α-CHCA) stock solution was prepared in 70% acetonitrile, 30% H_2O, and 0.1% TFA. An equal volume of 2 μM **BenzNP** solution was added to the matrix stock solution. 2.5 μL of this mixture was spotted on the sample carrier, and MALDI-MS analysis was performed on a Bruker Autoflex III mass spectrometer.

1.2.3 Dynamic light scattering. Hydrodynamic diameter and zeta potential of **BenzNP** was measured at 25°C by dynamic light scattering (DLS) in 5 mM phosphate buffer (pH=7.4) using a Malvern Zetasizer Nano ZS instrument. The measurement angle was 173° (backscatter). Data were analysed by the "multiple narrow modes" (high resolution) based on non-negative-least-squares (NNLS). 1 μM of **BenzNP** was placed in a cuvette and average of 3 measurements was considered.

1.2.4 Detailed protocol for the synthetic of the nanoparticle capping ligand (benzyl-ligand)

The following scheme describes the steps to synthesize the ligand covering **BenzNP**.

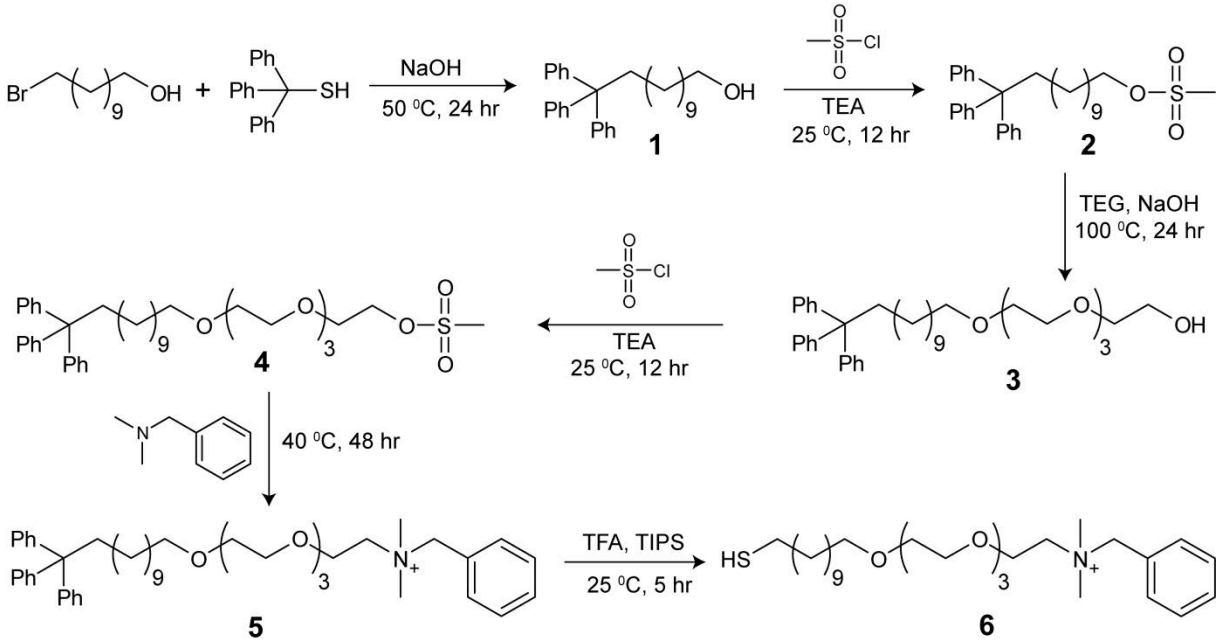

Supplementary Scheme 1. The scheme followed for synthesis of the benzyl-ligand **6** for functionalizing **BenzNP**.

Synthesis of compound 1: 11-bromo-1-undecanol (8.22 g, 32.74 mmol) was dissolved in 80 mL 1:1 ethanol/toluene mixture. Triphenylmethanethiol (10.86 g, 39.29 mmol) dissolved in 80 mL 1:1 ethanol/toluene was added to 11-bromo-1-undecanol in solution. Then, sodium hydroxide (1.96 g, 49.11 mmol) was dissolved in 2 mL water and added to the mixture. The reaction

mixture was stirred for 24 hours at 50°C. Upon completion, the reaction mixture was extracted twice with a saturated solution of sodium bicarbonate ($NaHCO_3$) The organic layer was extracted, dried over sodium sulfate (Na_2SO_4), and concentrated using a rotavapor. The crude product was purified by column chromatography over silica gel using hexane/ethyl acetate (1:1, v/v) as the eluent. The solvent was removed in vacuum to obtain compound **1** as colorless oil (yield: 13.88 g, 95%).

^{1}H NMR (400 MHz, $CDCl_3$, TMS) of Compound 1 : δ 7.48-7.40 (m, 6H, *HAr*-), 7.37-7.27 (m, 6H, *HAr*-), 7.26-7.18 (m, 3H, *HAr*-), 3.65 (t, *J* = 6.7Hz, 2H,***CH$_2$***OH), 2.16 (t, *J* = 7.2Hz, 2H,-***CH2-***), 1.66-1.52 (m, 2H, -SCH$_2$***CH$_2$***) , 1.44-1.12 (m, 16H, -***CH$_2$***CH$_2$OH + -***(CH$_2$)$_8$*** CH$_2$OH).

Synthesis of compound 2: Compound **1** (13.88 g, 31.1 mmol) in 150 mL dry dichloromethane (DCM) was mixed with triethylamine (TEA) (4.72g, 6.48 mL, 46.65 mmol), followed by dropwise addition of methanesulfonyl chloride (3.92 g, 2.65mL, 34.21 mmol) in ice bath. After 30 minutes the reaction mixture was warmed to room temperature and stirred for 12 hr. After the reaction was completed (by TLC), solvent was evaporated. The compound was diluted again with 100 mL DCM and extracted with 100 mL 0.1 M HCl twice. The organic layer was collected, neutralized with a saturated $NaHCO_3$ solution, and washed with water three times. Following extraction, the organic layer was dried over Na_2SO_4 and concentrated at reduced pressure. The crude product was purified by column chromatography over silica gel using hexane/ethyl acetate (1:1, v/v) as the eluent. Solvent was removed in vacuum to obtain the mesylated compound **2** as light yellow oil (yield: 15 g, 92%).

^{1}H NMR (400 MHz, $CDCl_3$, TMS) of Compound 2: δ 7.48-7.40 (m, 6H, *HAr*-), 7.34-7.27 (m, 6H, *HAr*-), 7.26-7.19 (m, 3H, *HAr*-), 4.24 (t, *J* = 6.8Hz, 2H, -***CH2***SO_3CH_3), 3.01 (s, 3H, -SO_3***CH$_3$***), 2.16 (t, *J* = 7.6Hz, -S***CH$_2$***-), 1.76 (p, *J* = 6.8Hz, 2H, -***CH2***CH2SO_3CH_3), 1.41 (p, *J* = 7.2Hz, 4H, -SCH2***CH$_2$***- + -SCH2CH$_2$***CH$_2$***-), 1.35-1.1 (m, 12H, -***(CH$_2$)$_6$*** $CH_2CH_2SO_3CH_3$).

Synthesis of compound 3: First, NaOH (1.37 g, 34.3 mmol) solution (1 mL) was added to 99.24 mL of tetraethyleneglycol (TEG) (111.15 g, 57.22 mmol) and stirred for 2 hr at 80 °C. To this reaction mixture, 15 g of 11-(tritylthio)undecyl methanesulfonate (compound **2**) was added and stirred for 48 hr at 100 °C. The product was extracted in hexane/ethyl acetate (4:1, v/v) six times. Then, the organic layer was concentrated at reduced pressure and the crude product was purified by column chromatography over silica gel using ethyl acetate as the eluent. The solvent was removed in vacuum to obtain compound **3** as light yellow oil (yield: 15.28 g, 68%).

^{1}H NMR (400 MHz, $CDCl_3$, TMS) of Compound 3: δ 7.47-7.40 (m, 6H, *HAr*-), 7.34-7.26 (m, 6H, *HAr*-), 7.25-7.19 (m, 3H, *HAr*-), 3.77-3.57 (m,16H, -CH_2-***(OCH$_2$CH$_2$)$_4$***-OH), 3.46 (t, *J* = 6.8 Hz, 2H, -***CH$_2$***-$(OCH_2CH_2)_4$-OH), 2.95 (br, s, 1H, -TEG-O**H**), 2.15 (t, *J* = 7.2Hz, -S***CH$_2$***-), 1.59 (p, *J* = 7.2Hz, 2H, -***CH$_2$***CH_2TEG-OH), 1.4 (p, *J* = 7.6Hz, 2H, -SCH2***CH$_2$***-), 1.35-1.13(m, 14H, -***(CH$_2$)$_7$*** CH_2CH_2TEG-OH).

Synthesis of compound 4: Triethylamine (3.26g, 4.49 mL, 32.2 mmol) was added to compound **3** (10 g, 16.1 mmol) in 100 mL dry DCM in an ice bath. Methanesulfonyl chloride (2.77 g, 1.87 mL, 24.1 mmol) was added dropwise to the reaction mixture in ice-bath. After 30 minutes the reaction mixture was warmed up to room temperature and stirred overnight. The reaction mixture was worked up and the organic layer was extracted. The extracted DCM layer was dried over Na_2SO_4 and concentrated at reduced pressure. The crude product was purified by column chromatography over silica gel using ethyl acetate as the eluent. Solvent was removed in vacuum to obtain compound **4** as light yellow oil (yield 10.7 g, 95 %).

^{1}H NMR (400 MHz, $CDCl_3$, TMS) of Compound 4: δ 7.44-7.37 (m, 6H, *HAr*-), 7.31-7.23 (m, 6H, *HAr*-), 7.22-7.16 (m, 3H, *HAr*-), 4.40-4.34 (m, 2H, -***CH$_2$***OSO_3CH_3), 3.78-3.54 (m, 14H, CH_2-***(OCH$_2$CH$_2$)$_3$-CH$_2$***$CH_2OSO_3CH_3$), 3.44 (t, *J* = 6.8Hz, 2H, CH_2-***CH$_2$***-$(OCH_2CH_2)_3$-), 3.07 (s,

3H, -OSO_3***CH_3***), 2.12 (t, *J* = 7.2Hz, 2H, -S***CH_2***-), 1.56 (p, *J* = 7.2Hz, 2H, -***CH_2***CH_2TEG-$N(CH_3)_2$), 1.38 (p, *J*=7.6Hz, 2H, -SCH2***CH_2***-), 1.32-1.11 (m, 14H, -***$(CH_2)_7$***CH_2CH_2TEG).

Synthesis of compound 5: Compound **4** (1.075 g, 1.53 mmol) was added to dimethylbenzylamine (0.62 g, 0.7 ml, 4.6 mmol) in 10 mL ethanol. The reaction mixture was stirred at 40 ^oC for 48 hr. After evaporating ethanol at reduced pressure, the light yellow residue was purified by successive washings with hexane (10 mL, 4 times) and hexane/diethylether (1:1 v/v, 10 mL, 6 times) and then dried in high vacuum. The product formation was quantitative and was confirmed by NMR spectroscopy.

^{1}H NMR (400MHz, $CDCl_3$, TMS) of Compound 5: δ 7.64-7.58 (m, 2H, *HAr*-), 7.38-7.32 (m, 9H, *HAr*-), 7.24-7.17 (m, 6H, *HAr*-), 7.16-7.09 (m, 3H, *HAr*-), 4.9 (s, 2H, -***CH_2***-C_6H_5), 3.94 (s, br, 2H, -O***CH_2***$CH_2N(CH_3)_2$-), 3.8 (s, br, 2H, -OCH_2***CH_2***$N(CH_3)_2$-), 3.77-3.22 (m, 12H, -***$(OCH_2CH_2)_3$***-$CH_2CH_2N(CH_3)_2$-), 3.33 (t, *J* = 6.8Hz, 2H, -CH_2***CH_2***O-), 3.23 (s, 6H, -N***$(CH_3)_2$***-), 2.06 (t, *J* = 7.2Hz, 2H, -S***CH_2***-), 1.51-1.42 (p, *J* = 6.8Hz, 2H, -***CH_2***CH_2O-), 1.36-1.28 (p, *J* = 7.6Hz, 2H, -SCH2***CH_2***-) 1.24-1.08 (m, 14H, -***$(CH_2)_7$*** CH_2CH_2O-).

Synthesis of compound 6: An excess of trifluoroacetic acid (TFA, 20 equivalents, 3.69 g, 2.5 mL, 32.4 mmol) was added to compound **5** (1.2 g, 1.62 mmol) in 10 mL dry DCM. The color of the solution turned yellow upon addition of TFA. Then, triisopropylsilane (TIPS, 3 equivalents, 0.77g, 1 mL, 4.86 mmol) was added to the reaction mixture. The reaction mixture was stirred for 12 hr under N_2 at room temperature. The solvent, most of TFA, and TIPS were evaporated under reduced pressure. The yellow residue was purified by repeated washing with hexane (10 mL, 4 times) and dried in high vacuum. The final product formation was quantitative and was confirmed by NMR spectroscopy.

^{1}H NMR (400 MHz, $CDCl_3$, TMS) of Compound 6: δ 7.57-7.47 (m, 5H), 4.61 (s, 2H, -***CH_2***-C_6H_5), 4.01 (s, br, 2H, -O***CH_2***$CH_2N(CH_3)_2$-), 3.74-3.48 (m, 14H, -***$(OCH_2CH_2)_3$***-

$CH_2\mathbf{CH_2}N(CH_3)_2$-), 3.41 (t, *J* = 6.8Hz, 2H, -CH_2***CH_2***O-), 3.14 (s, 6H, -N***$(CH_3)_2$***-), 2.52 (q, *J* = 7.2Hz, HS***CH_2***-), 1.65-1.48 (m, 4H, -***CH_2***CH_2O-,+ HSCH2***CH_2***-), 1.43-1.20 (m, 15H, -***$(CH_2)_7$*** CH_2CH_2O- + ***H***S-).

1.2.5 Synthesis of benzyl-ligand protected gold nanoparticle (BenzNP)

We followed two-step method for synthesizing **BenzNP**, where a gold nanoparticle core was synthesized followed by place-exchange with the ligand of interest. First, pentanethiol-coated AuNPs with core diameter ~2 nm were synthesized using the Brust-Schiffrin two-phase synthesis protocol[7,8]. Subsequently, Murray place-exchange[9] method was followed to obtain the benzyl-ligand protected AuNPs. Pentanethiol conjugated AuNPs (10 mg) and compound **6** (27 mg) was dissolved in a mixture of 5 mL dry DCM, and 1 mL methanol and stirred under nitrogen atmosphere for 72 hr at room temperature. Then, solvents were removed under reduced pressure and the resulting precipitate was washed with hexane (10 mL) three times and with DCM (10 mL) twice. Then the precipitate was dissolved in distilled water and dialyzed for 72 hr (membrane molecular weight cut-off =10,000) to remove excess ligands, pentanethiol, acetic acid, and other salts present in the nanoparticle solution. After dialysis, the particle was lyophilized to yield a solid brownish product. The particles were then redispersed in deionized water (Milli-Q, Millipore). ^{1}H NMR-spectra in D_2O showed substantial broadening of the proton peaks with no sign of free ligands. The particle was further characterized by transmission electron microscopy, MALDI-MS, and DLS (Supplementary Fig. 1, 2, and 3, respectively).

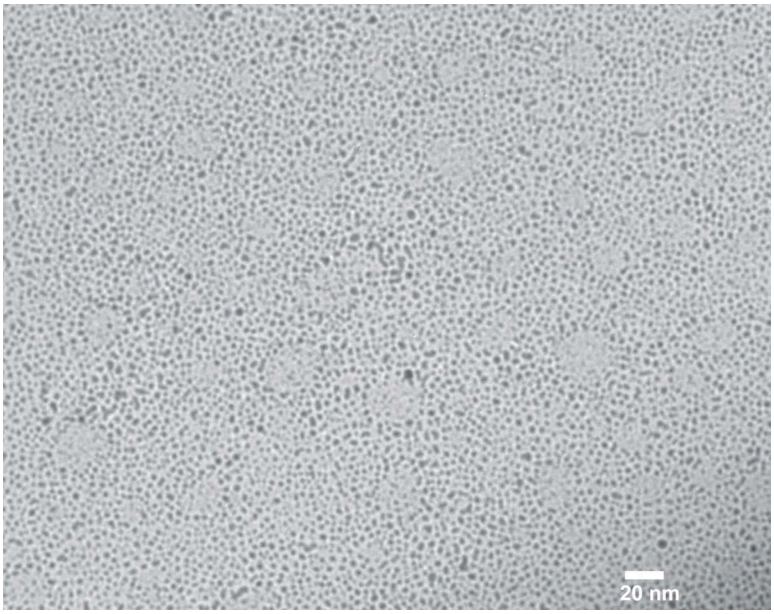

Supplementary Figure 1. Transmission electron micrograph of BenzNP.

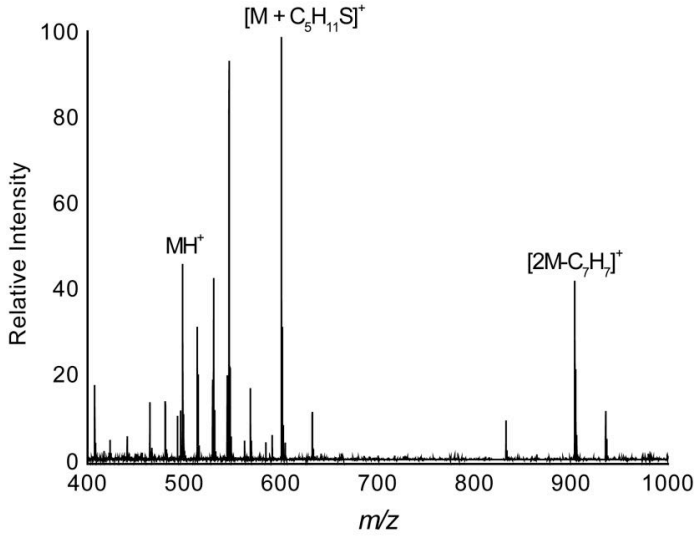

Supplementary Figure 2. MALDI-MS spectrum of BenzNP. The molecular ion (MH^+, *m/z* =498) was detected, and the disulfide ion formed by the benzyl ligand and the original pentanethiol was also detected at *m/z* 600.

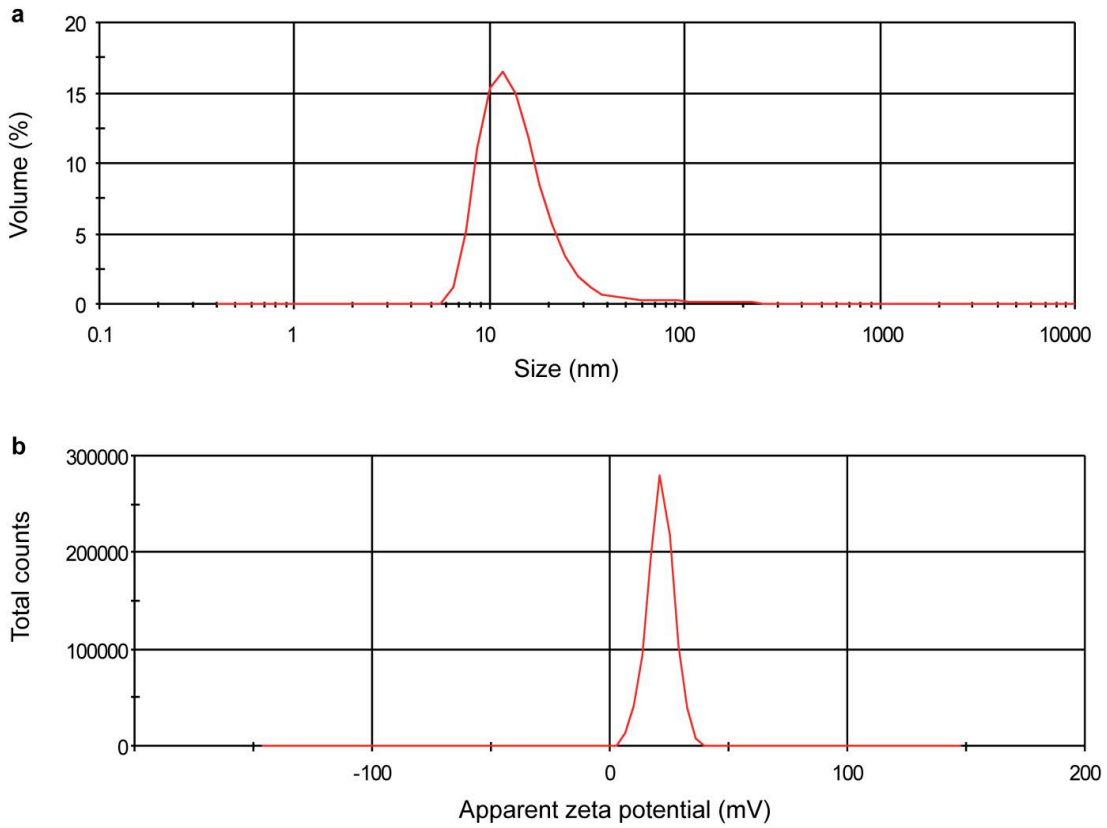

Supplementary Figure 3. Characterization of BenzNP. (**a**) Size (diameter) of **BenzNP** was measured by DLS from three independent experiments. The hydrodynamic diameter of the **BenzNP** is 17.6 ± 1.2 nm. (**b**) Zeta potential of **BenzNP** was measured by DLS. The overall charge of **BenzNP** is measured as 25.5 ± 1 mV from three independent replicates.

Section 2: Sensor Fabrication

2.1 Fluorescence titrations. In the fluorescence quenching experiment, an equimolar solution of the three FPs (100 nM each) was titrated with various concentrations of **BenzNP** ranging from 0 to 300 nM. The excitation/emission/cut-off wavelengths were 380/450/435, 475/510/495, and 550/585/570 nm for EBFP2, EGFP and tdTomato, respectively. The change of fluorescence intensity at the respective emission maxima was recorded on a Molecular Devices SpectraMax M3 microplate reader at 25 ^{0}C. Decay of fluorescence intensity of each FP was observed with

increasing NP concentration. Nonlinear least-squares curve fitting analysis was employed to estimate the binding constant (K_a) and association stoichiometry (n) using a 1:1 binding model[10,11].

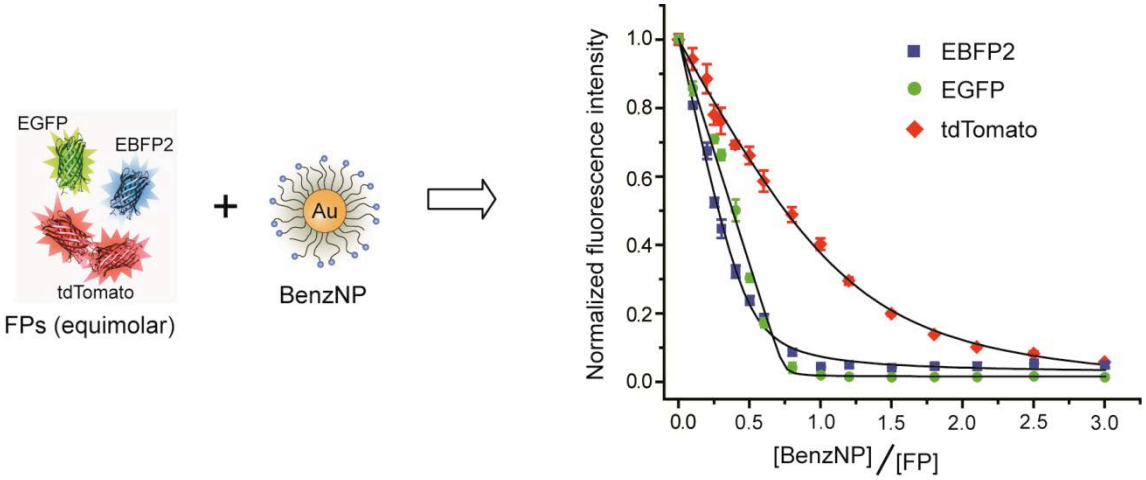

Supplementary Figure 4. Titration of FPs with BenzNP. Fluorescence titration of an equimolar mixture of the three FPs by **BenzNP**. The emissions for each FP were measured independently at the corresponding emission wavelengths. The data points are averages of three replicates and the error bars represent the standard deviations. The black solid lines through the data points represent the best curve fitting using the model of single set of identical binding sites.

Supplementary Table 1. Binding parameters for the **BenzNP**-FP complexes as determined by the fitting of the fluorescence titration curves.

Protein	**Binding constant (K_a), M^{-1}**	**Binding ratio (n)**	**R^2**
EBFP2	$(1.66 \pm 0.5) \times 10^8$	2.0 ± 0.09	0.99641
EGFP	$(9.26 \pm 2.8) \times 10^9$	1.3 ± 0.03	0.99508
tdTomato	$(6.69 \pm 2.6) \times 10^7$	0.8 ± 0.04	0.99678

2.2 Sensor preparation: First, a FP solution was prepared by mixing the FPs at the final concentration of 100 nM (for each FP). The **BenzNP**-FP sensor was generated by incubating the

FP solution with **BenzNP** (at the final concentration of 150 nM) for 30 min in 5 mM sodium phosphate buffer (pH 7.4). The FP and **BenzNP**-FP solutions were maintained in the dark to minimize photobleaching of the FPs, if any. This conjugate was then added to the drug-treated cells for screening studies.

Section 3: Drug Screening

3.1 Cell culture. BT549 cell line was purchased from ATCC (ATCC® HTB-122™). pTD cell line[12] was generously donated by Prof. D. Josph Jerry. BT549 cells were cultured in DMEM media supplemented with 10% FBS and 1% antibiotics. Cells were grown in a humidified atmosphere containing 5% CO_2 at 37^0C. The TD cells were cultured in DMEM high glucose media supplemented with 10% FBS and 1% antibiotics. At ~80% confluence, cells were trypsinized and plated in 96-well plates (Greiner black-and-clear bottom) and cultured for the next studies.

3.2 IC_{50} of the drugs. The IC_{50} values of the drugs were determined by alamar blue assay. Cells were seeded at 10,000 (for BT549 cells) or 15,000 (for pTD cells) cells/well in 96-well microplates (Greiner black-and-clear bottom). After 24 hours, the cells were washed twice with phosphate buffered saline (PBS) and treated with the drugs at different concentrations. The drug treatment was continued for 24 hours for all the drugs except hydrogen peroxide and sodium nitroprusside for which a 5 hour treatment was effective. Drug treatment was done in cell culture media lacking antibiotics. After the drug treatments, cells were washed with PBS twice and the percentage cell viability was determined by using Alamar blue assay following the manufacturer's protocol (Invitrogen). The IC_{50} values were determined by fitting the data using a

dose response model with variable Hill slope built in OriginPro version 8.5 (Supplementary Fig. 5, and Supplementary Table 3 – 4).

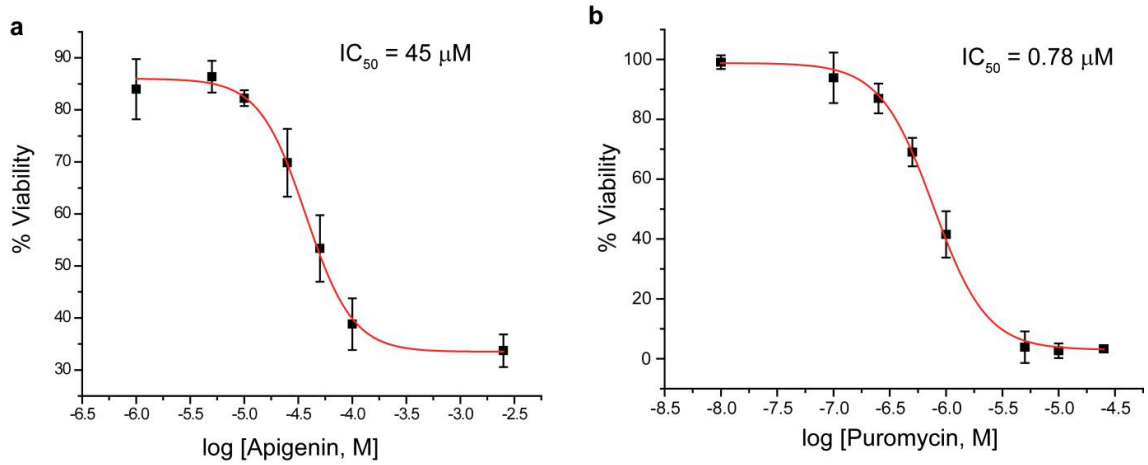

Supplementary Figure 5. Determination of IC_{50} value of the single cytotoxic compounds. Representative dose response curves of **a,** apigenin, and **b,** puromycin using 10,000 BT549 cells after 24 hours of drug treatment. The IC_{50} values were determined by fitting the data (the red line) using dose response model with variable Hill slope built in Origin 8.5 program.

Supplementary Table 2. Concentrations used for determining the IC_{50} values of PUR-CSP combinations. The concentrations were the same for combinations of PUR-APG and APG-CSP.

Total drug conc. (μM)		0	0.01	0.5	1	5	10	25	50	100	250	500
PUR-CSP (1:1)	PUR (μM)	0	0.005	0.25	0.5	2.5	5	12.5	25	50	125	250
	CSP (μM)	0	0.005	0.25	0.5	2.5	5	12.5	25	50	125	250
PUR-CSP (1:3)	PUR (μM)	0	0.0025	0.125	0.25	1.25	2.5	6.25	12.5	25	62.5	125
	CSP (μM)	0	0.0075	0.375	0.75	3.75	7.5	18.75	37.5	75	187.5	375
PUR-CSP (3:1)	PUR (μM)	0	0.0075	0.375	0.75	3.75	7.5	18.75	37.5	75	187.5	375
	CSP (μM)	0	0.0025	0.125	0.25	1.25	2.5	6.25	12.5	25	62.5	125

Dose response studies for combination of drugs were followed in a similar method of single drug. Three drugs (puromycin (PUR), cisplatin (CSP), and apigenin (APG)) were chosen arbitrarily to study the drug combinations (Fig. 4). To determine the IC_{50} values, two drugs of a

combination were added to confluent cells one by one at 1:1, 1:3, and 3:1 ratios with varying concentrations (Supplementary Table 2). The concentrations of drugs used were same for all the different combinations (PUR-CSP, PUR-APG, and APG-CSP). The IC_{50} values were determined by fitting the data using the same dose response model (Supplementary Fig. 6 and Supplementary Table 5).

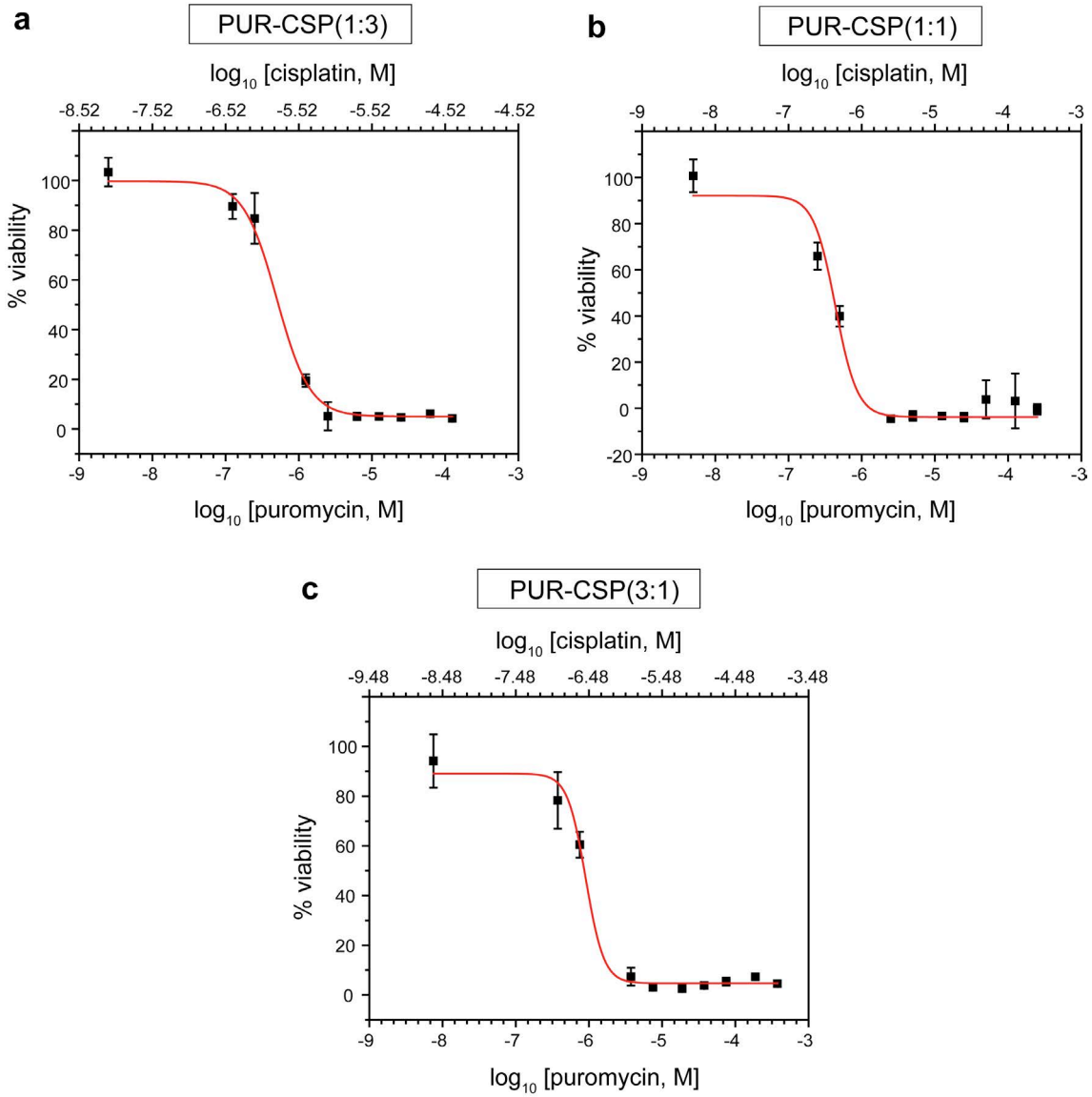

Supplementary Figure 6. Determination of IC_{50} value of the combination of drugs. Representative dose response curves of the drug combinations **a**, PUR-CSP(1:3), **b**, PUR-

CSP(1:1), and **c**, PUR-CSP(3:1) using 10,000 BT549 cells after 24 hours of drug treatment. The IC_{50} values were determined by fitting the data (the red line) using dose response model with variable Hill slope built in Origin 8.5 program. The IC_{50} concentrations are reported in Supplementary Table 5.

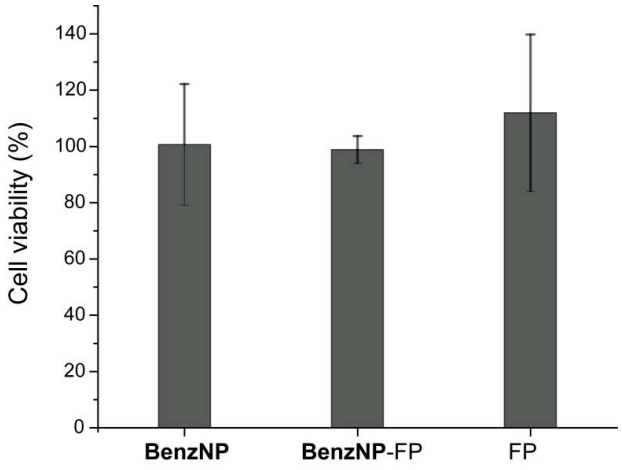

Supplementary Figure 7. Cell viability of the sensor elements. Cell viability was determined using alamar blue assay after incubating 10,000 BT549 cells with **BenzNP**, **BenzNP**-FP, and only FP for 15 minutes.

3.3 Drug screening studies. The drugs were purchased from VWR International, Sigma-Aldrich, and Tocris Bioscience. First, 10,000 (for BT549 cells) or 15,000 (for pTD cells) cells/well were seeded in 96-well Greiner black-and-clear bottom microplates and allowed to grow in their respective culture media at 37°C and 5% CO_2 for 24 hours. Then, cells were washed twice with PBS and treated with the drugs at their respective IC_{50} values (Supplementary Table 2, 3, and 5). The drug treatment was continued for 24 hours for the individual drugs as well as their combinations (except for hydrogen peroxide and sodium nitroprusside, which were treated for 5 hours). Cells were then washed three times with PBS and incubated with the sensor for 15 minutes before taking the reading.

Then, 200 µL of the **BenzNP**-FP conjugate was loaded into 96-well plates containing drug treated cells to be analyzed. After 15 mins of incubation with the sensor, fluorescence intensities were monitored for each FP using a plate reader (Molecular Device Spectramax M3) at 25°C. Appropriate filters were used to collect emissions from each FP. The excitation/emission/cut-off wavelengths were 380/450/435, 475/510/495, and 550/585/570 nm for EBFP2, EGFP and tdTomato, respectively. Fluorescence responses were $\log_2$-transformed (Supplementary Table 7 – 12) before employing the statistical analyses.

Supplementary Table 3. Description of the test compounds screened in the study using BT549 cell line.

* denotes the drugs that were included in the reference set.

	Drug name	Drug mechanism	Drug target(s)	Drug type	Drug class	IC_{50} (µM)	Pubchem ID
1	Daunorubicin HCl*	topoisomerase II inhibition	topoisomerase II	small molecule	chemo-therapeutic	1.7	30323
2	Etoposide*	topoisomerase II inhibition	topoisomerase II	small molecule	chemo-therapeutic	90	36462
3	Apigenin	topoisomerase II inhibition	topoisomerase II	natural product	in clinical development	45	5280443
4	Doxorubicin HCl*	topoisomerase II inhibition	topoisomerase II	small molecule	chemo-therapeutic	7	31703
5	6-Thioguanine*	DNA methylation memetic	DNA methylation	small molecule	experimental	250	2723601
6	Temozolomide*	DNA methylation	DNA methylation	small molecule	chemo-therapeutic	120	5394
7	Thio-TEPA	DNA alkylation	DNA alkylation	small molecule	chemo-therapeutic	180	5453
8	Cisplatin*	DNA crosslinking	DNA crosslinking	small molecule	chemo-therapeutic	86	5702198
9	Oxaliplatin	DNA crosslinking	DNA crosslinking	small molecule	chemo-therapeutic	140	5310940

10	Chlorambucil*	DNA crosslinking	DNA crosslinking	small molecule	chemo-therapeutic	605	2708
11	Paclitaxel	disruption of mitosis	microtubules	natural product	chemo-therapeutic	0.012	36314
12	Vinblastin sulfate*	disruption of mitosis	microtubules	natural product	chemo-therapeutic	0.012	6710780
13	Vincristine sulfate*	disruption of mitosis	microtubules	natural product	chemo-therapeutic	0.01	249332
14	Anisomycin	protein synthesis inhibition	antibiotic	natural product	experimental	0.4	253602
15	Emetine	protein synthesis inhibition	antibiotic	natural product	clinical	0.2	10219
16	Puromycin	protein synthesis inhibition	antibiotic	natural product	experimental	0.78	439530
17	Roscovitine*	CDK inhibition	CDKs	small molecule	in clinical development	0.06	160355
18	Purvalanol A	CDK inhibition	CDKs	small molecule	experimental	4.64	456214
19	Olomoucine*	CDK inhibition	CDKs	small molecule	experimental	117	4592
20	Apicidin*	HDAC inibition	HDAC	natural product	experimental	7	15489645
21	Vorinostat*	HDAC inibition	HDAC	small molecule	clinical	160	5311
22	Scriptaid	HDAC inibition	HDAC	small molecule	experimental	19	5186
23	Hydrogen peroxide*	necrosis	necrotic	small molecule	experimental	480	784
24	Sodium nitroprusside*	necrosis	necrotic	small molecule	experimental	450	11963622
25	β-lapachone	necrosis	necrotic	small molecule	in clinical development	0.65	3885
26	ALLN	protein degradation	proteasome	small molecule	experimental	7.1	4332
27	MG-132	protein degradation	proteasome	small molecule	experimental	0.8	462382
28	Irinotecan	topoisomerase I inhibition	topoisomerase I	small molecule	chemo-therapeutic	20	60838
29	Topotecan	topoisomerase I inhibition	topoisomerase I	small molecule	chemo-therapeutic	52	60700

CDK: cyclin-dependent kinase; HDAC: histone deacetylase

Supplementary Table 4. Description of the chemotherapeutic candidates screened in the study using pTD cell line.

	Drug name	Drug mechanism	Drug target(s)	Drug type	Drug class	IC_{50} (µM)	Pubcehm ID
1	Doxorubicin HCl	Topoisomerase II inhibition	Topoisomerase II	Small molecule	Chemo-therapeutic	1	31703
2	Daunorubicin HCl	Topoisomerase II inhibition	Topoisomerase II	Small molecule	Chemo-therapeutic	1.5	30323
3	6-Thioguanine	DNA methylation memetic	DNA methylation	small molecule	experimental	5	2723601
4	Gemcitabine	Nucleic acid synthesis inhibition	Nucleic acid synthesis	small molecule	chemo-therapeutic	0.09	60750
5	Cisplatin	DNA crosslinking	DNA crosslinking	small molecule	chemo-therapeutic	12	5702198
6	Chlorambucil	DNA crosslinking	DNA crosslinking	small molecule	chemo-therapeutic	250	2708
7	Carboplatin	DNA crosslinking	DNA crosslinking	small molecule	chemo-therapeutic	340	10339178
8	Paclitaxel	disruption of mitosis	microtubules	natural product	chemo-therapeutic	5	36314
9	Vinblastin sulfate	disruption of mitosis	microtubules	natural product	chemo-therapeutic	5	6710780
10	Vincristine sulfate	disruption of mitosis	microtubules	natural product	chemo-therapeutic	1	249332
11	Hydrogen peroxide	necrosis	necrotic	small molecule	experimental	100	784
12	Sodium nitroprusside	necrosis	necrotic	small molecule	experimental	500	11963622
13	Camptothecin	topoisomerase I inhibition	topoisomerase I	natural product	chemo-therapeutic	1	104842
14	Irinotecan	topoisomerase I inhibition	topoisomerase I	natural product	chemo-therapeutic	5	60838

Section 3: Determination of FICI

Supplementary equation 1. The fractional inhibitory concentration index (FICI) was calculated using the following equation[13] based on Loewe additivity[14,15]:

$$FICI = \frac{[A]_C}{[A]_E} + \frac{[B]_C}{[B]_E}$$

where, $[A]_C$ and $[B]_C$ are the concentrations of drug A and B in the combination associated with a particular level of effect, e.g., IC_{50}, and $[A]_E$ and $[B]_E$ are the concentrations of A and B when used singly to produce the same level of effect. FICI < 1 indicates synergism, while 1 ≤ FICI < 4 indicates additivity, and FICI ≥ 4 indicates antagonism[13].

Supplementary Table 5. Fractional inhibitory concentration of drug candidates and their combinations using BT549 cells. Cells were simultaneously treated with the drugs for 24 h at the ratios indicated (three replicates for each). Dose response curves for the individual drugs and the combinations were determined by Alamar blue assays and the IC_{50} concentrations were obtained from curve fitting. The FICI values of the drugs were calculated according to Supplementary Equation 1 using the IC_{50} values. The therapeutic activities were inferred from the conditions set in the equation.

Drugs	Concentration @ IC_{50} of the combination (μM)		FICI	Action
	Drug A	Drug B		
APG	45	-	N/A	N/A
CSP	86	-	N/A	N/A
PUR	0.78	-	N/A	N/A
APG-CSP (1:1)	34.5	34.5	1.17	Additive
APG-CSP (1:3)	15.5	46.5	0.89	Synergistic
APG-CSP (3:1)	9	3	0.23	Synergistic
PUR-APG (1:1)	0.65	0.65	0.85	Synergistic
PUR-APG (1:3)	0.8	2.4	1.08	Additive
PUR-APG (3:1)	0.6	0.2	0.77	Synergistic
PUR-CSP (1:1)	0.4	0.4	0.52	Synergistic
PUR-CSP (1:3)	0.525	1.575	0.69	Synergistic
PUR-CSP (3:1)	1.825	0.275	1.06	Additive

Section 4: Statistical Methods

4.1 Hierarchical clustering analysis. Hierarchical clustering analysis (HCA) of the average data set was performed using the *hclust* function of the stats package of R assuming a complete linkage method[16]. *hclust* begins with each case serving as its own cluster; at each step in the clustering process, the two most similar cases or clusters are joined; the process iterates until all cases fall into a single cluster. HCA allows cases with mechanisms outside the reference set to be identified as novel, if they are dissimilar from the other cases in the set; in this case, they are linked to the other cases/clusters relatively high in the denodrogram.

4.2 Linear discriminant analysis. The raw fluorescence response data matrix was processed by classical linear discriminant analysis (LDA) using SYSTAT software (version 11.0, SystatSoftware, Richmond, CA, USA). In LDA, all variables were used in the model (complete mode) and the tolerance was set as 0.001. The raw fluorescence response patterns were transformed to canonical patterns where the ratio of between-class variance to the within-class variance was maximized, where the classes were defined as the drug mechanisms in the reference set. This defines the LDA solution space.

To identify the unknown (blinded) samples, we first re-ran LDA on the reference set using the *lda* function in the MASS package[17] of R; these results replicated the SYSTAT analysis. Predicted classifications for the blinded samples were then obtained using the *predict.lda* function that uses the fluorescence response patterns of each new case to compute the Mahalanobis distance of that case to the centroid of each mechanism cluster in the LDA solution space (Fig. 3b). Blinded cases are predicted to belong to the closest mechanism class, defined by the shortest Mahalanobis distance. Because some distance is always shortest, LDA is incapable of identifying blinded or completely unknown samples as having novel mechanisms. However,

by considering the expected distribution of Mahalanobis distances under these conditions, cases can be identified as outliers if they fall far from the closest centroid (i.e., have an associated *p*-value < 0.01). Here, the distances are proportional to an *F* distribution[18]: for *n* cases overall, *p* dimensions in the LDA solution and Mahalanobis distances d^2,

$$\frac{nd^2(n-p)}{p(n-1)(n+1)} \sim F(p, n-p).$$

Supplementary Table 6. Leave-one-out analysis by Jackknifing in linear discriminant analysis. Each mechanism group contains drugs with 8 replicates as in the reference set.

	I	II	III	IV	V	VI	VII	**% correct**
I	16	0	0	0	0	0	0	100
II	0	16	0	0	0	0	0	100
III	0	0	24	0	0	0	0	100
IV	0	0	0	15	0	1	0	94
V	0	0	0	0	16	0	0	100
VI	0	0	0	0	0	16	0	100
VII	0	0	0	0	0	0	16	100
Total	16	16	16	15	16	17	16	**99**

I : disruption of mitosis (vinblastin sulfate, vincristine sulfate);
II : HDAC inhibition (apicidin, vorinostat);
III : topoisomerase II inhibition (daunorubicin HCl, etoposide, doxorubicin HCl);
IV : DNA methylation (6-thioguanine, temozolomide);
V : CDK inhibition (roscovitine, olomoucine);
VI : DNA crosslinking (cisplatin, chlorambucil);
VII : necrosis (sodium nitroprusside, hydrogen peroxide)

4.3 Robustness of the classification approach. Leave-one-out cross-validation using Jackknifed analysis on the reference set was performed (Supplementary Table 6) in SYSTAT to investigate the reliability of LDA approach for classifying the drugs. The analysis successively classifies all cases but one to develop a discriminant function and then categorizes the case that was left out.

This process is repeated with each case left out in turn. To assess the classification of unknown cases based on the shortest Mahalanobis distance, the distribution of all the distances was investigated. The distribution of squared Mahalanobis distances between each drug mechanism from the training set and blinded unknowns were plotted (Supplementary Fig. 8) as cumulative density functions (CDF) using the *cdfplot* function in StataSE 13. CDFs were also prepared for those drugs identified as novel mechanisms (Supplementary Fig. 9).

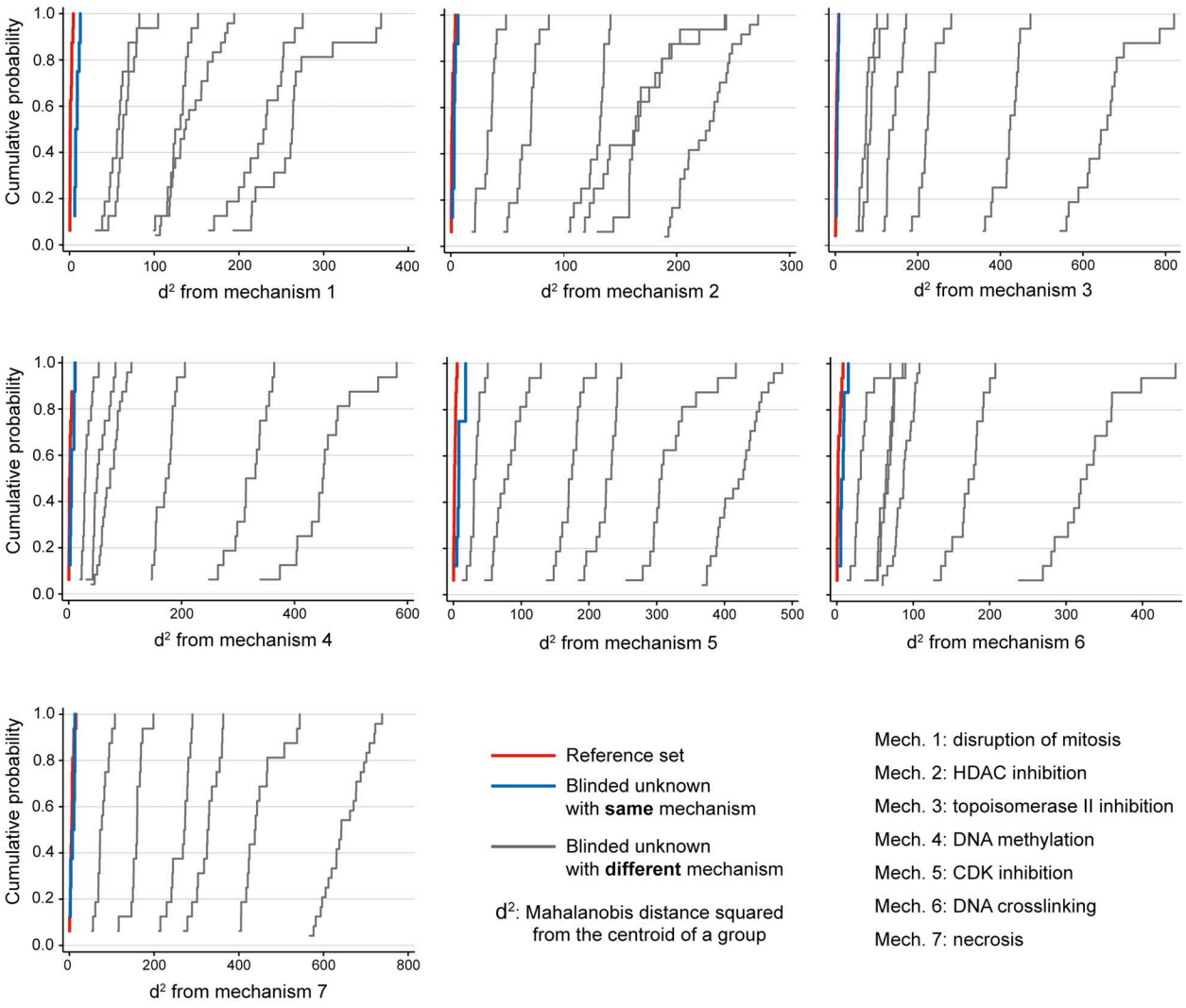

Supplementary Figure 8. Cumulative density functions for the squared Mahalanobis distance between blinded unknowns and each mechanism from the reference set.

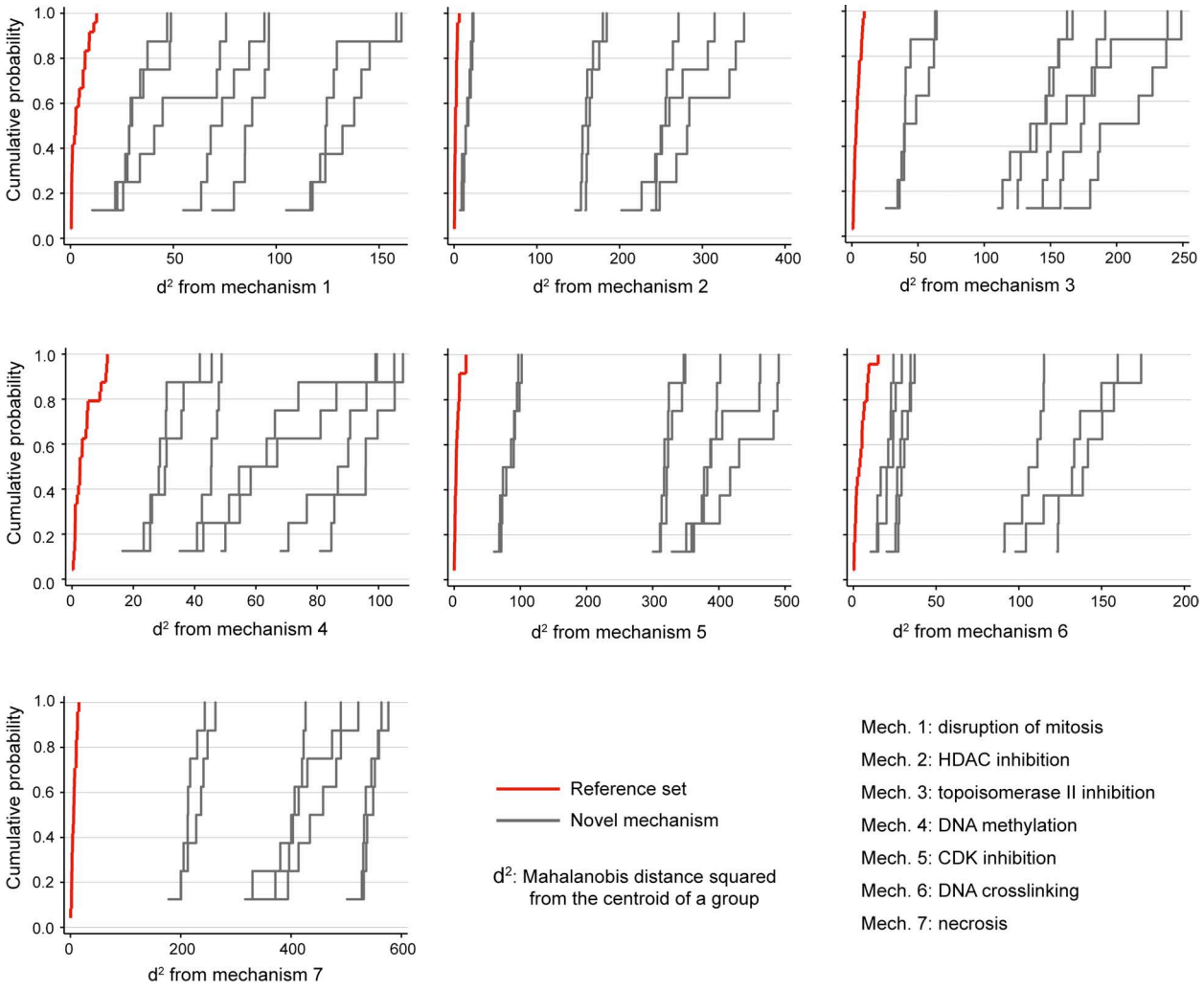

Supplementary Figure 9. Cumulative density functions for the squared Mahalanobis distance between novel mechanisms and each mechanism from the reference set.

It is observed that the distribution of the distances of the blinded unknowns from the reference set are clearly and considerably shorter for those drugs correctly identified as belonging to a given mechanism. Similarly, the large separation between novel mechanisms and each drug mechanism in the reference set further supports the use of the shortest Mahalanobis distance for correctly classifying unknown cases.

Section 5: Validation of the Drug Screening Methodology

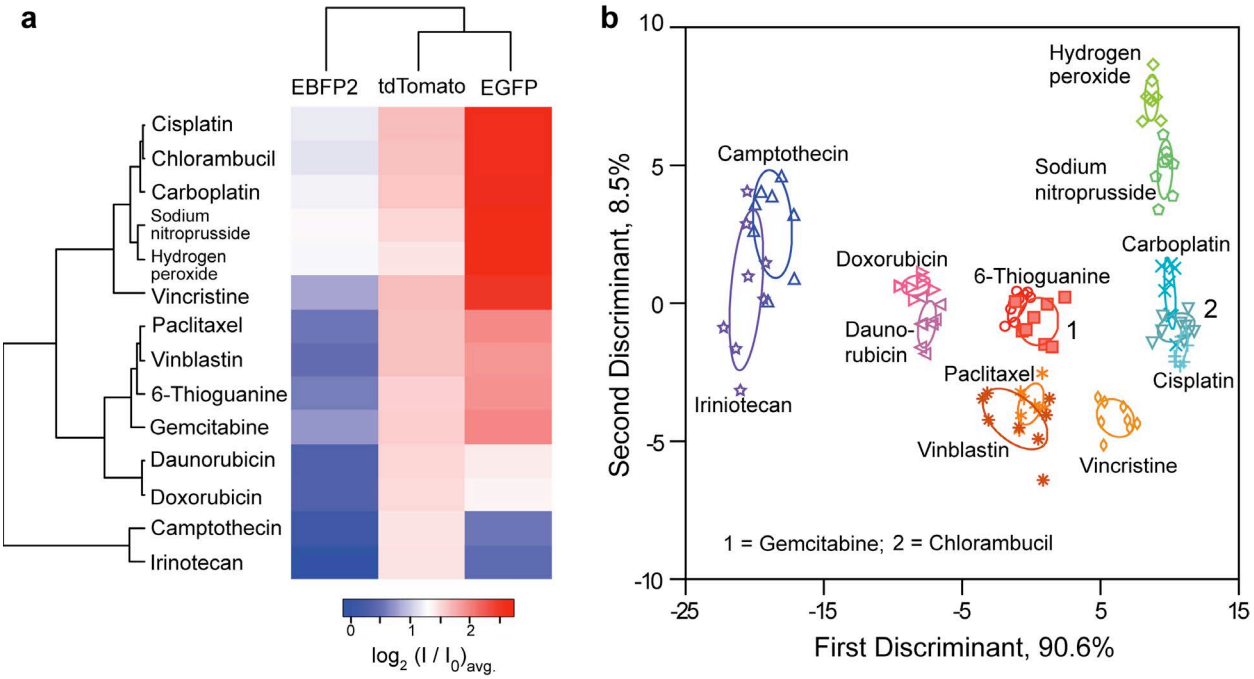

Supplementary Figure 10. Drug screening using pTD cells. **a**, Heat map of the fluorescence responses pTD cells when treated with 11 reference drugs, where I_0 and I are respectively the fluorescence before and after the addition of the sensor to the cells. Agglomerative hierarchical analysis was performed on the averages of the fluorescence responses. The dendrogram shows degree of association. **b,** Linear discriminant analysis of the fluorescence responses resulted in canonical scores with three discriminants explaining 90.6, 8.5, and 0.9% of total variance and plotted with 95% confidence ellipses around the centroid of each group (based on the standard error of the mean).

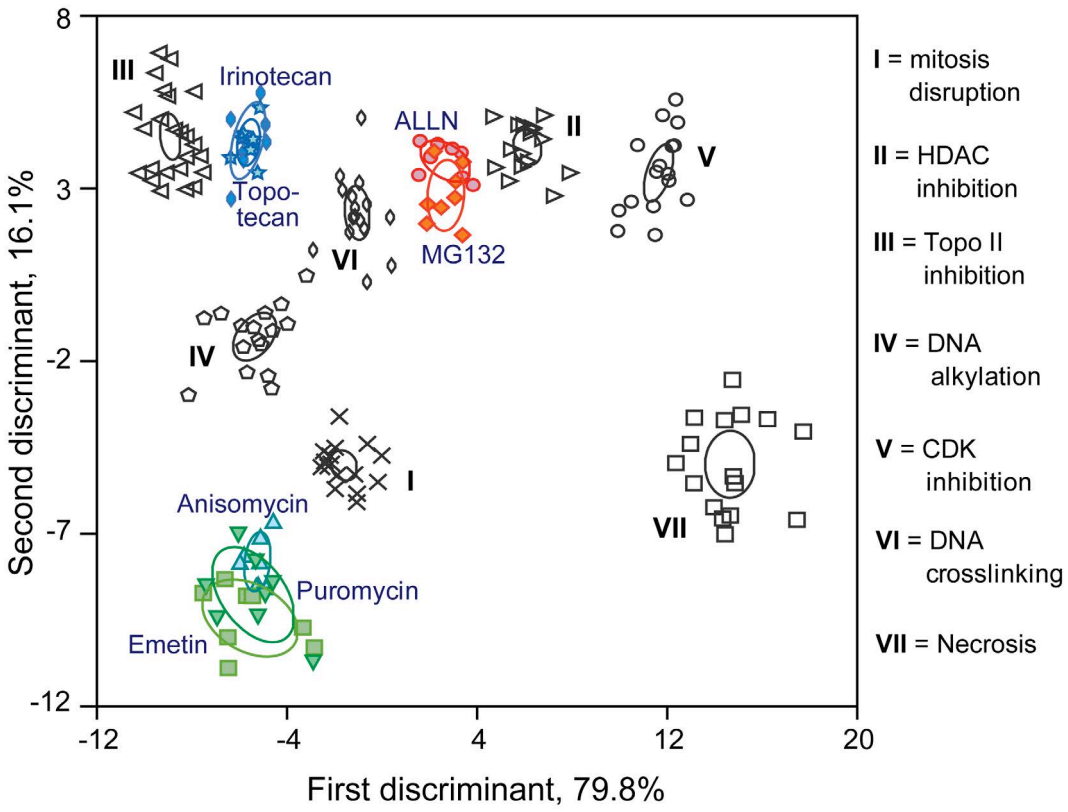

Supplementary Figure 11. Classification of unknowns outside the initial reference set using BT549 cells. Updated canonical score plot was derived from LDA of the fluorescence responses from a combination of the initial reference set and the compounds with 'novel' mechanisms, and were plotted with 95% confidence ellipses around the centroid of each group (based on the standard error of the mean). The clusters corresponding to the 'novel' compounds are colored, while the initial reference set compounds are presented in black.

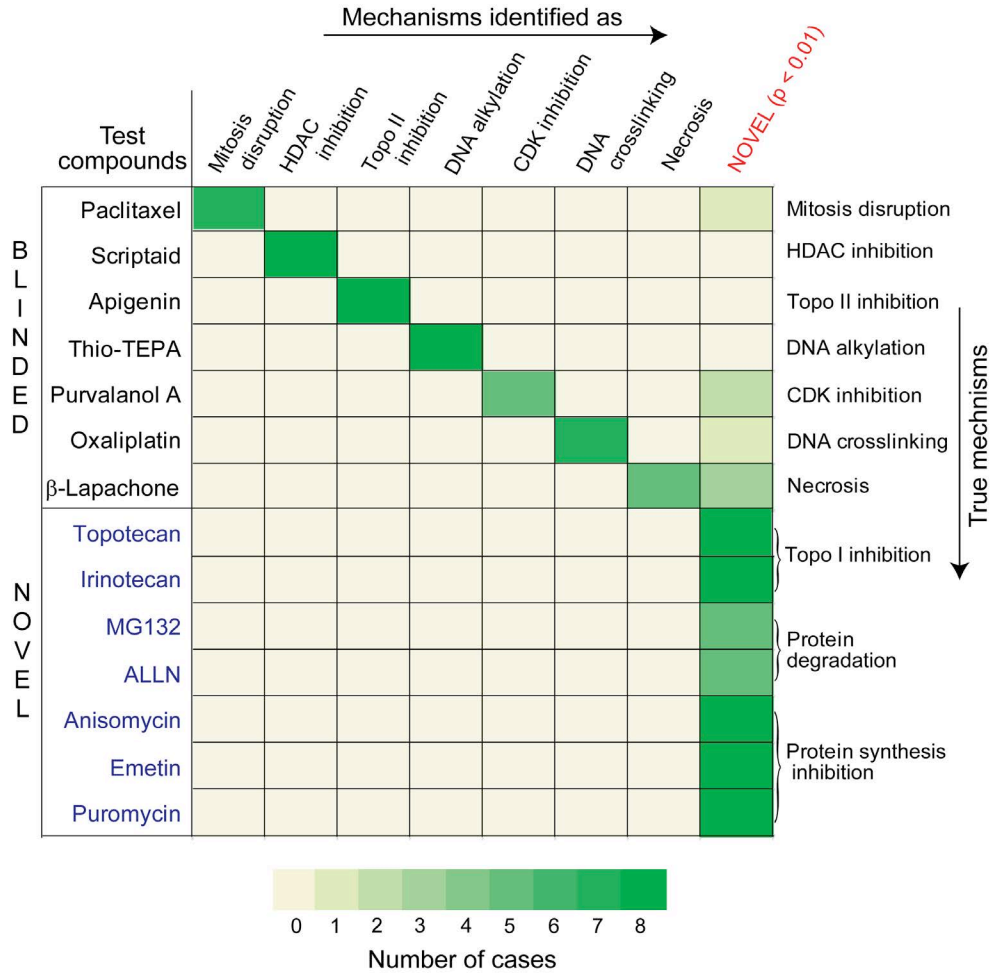

Supplementary Figure 12. Prediction of drug mechanisms on parallel replicates using the triple-channel sensor. Fluorescence responses from the EBFP2, EGFP, and tdTomato channels were utilized to perform the statistical analysis. The *p*-values were derived from *F*-distribution on the minimum Mahalanobis distance of each replicate to the centroid of reference groups calculated by LDA. Based on the *p*-values, each unknown case (parallel replicate) was assigned to a mechanistic group of the reference set or regarded as 'novel'. The blinded unknowns exhibits cell death mechanisms similar to the reference set, while the 'novel' unknowns involve mechanisms completely different from the reference set.

Supplementary Table 7. Identification of unknowns using BT549 cells. The average fluorescence responses ($log_2(I / I_0)_{avg.}$) of eight replicates for each drug was analyzed by LDA specifying the drug identities that are listed on top of the table (from known literature reported mechanisms). Using the shortest Mahalanobis distance of a case from the centroid of the reference groups, *p*-values were calculated. A threshold *p*-value of 0.01 determined if a test case was adjacent to a reference group. A *p*-values <0.01 was considered to be indicative of "novel" mechanism.

Identities: 1 = disruption of mitosis; 2 = HDAC inhibition; 3 = topoisomerase II inhibition; 4 = DNA alkylation; 5 = CDK inhibition; 6 = DNA crosslinking; 7 = necrosis; 8 = topoisomerase I inhibition; 9 = protein degradation; 10 = protein synthesis inhibition; where 8, 9, and 10 are the "novel" mechanistic groups.

Drug name	$log_2(I / I_0)_{avg.}$			Identity	Shortest Mahalanobis distance	*p*-value	Correct prediction
	EBFP2	EGFP	tdTomato				
Paclitaxel	0.474453	1.849425	0.885746	1	7.735	0.06	yes
Scriptaid	1.32178	2.295043	1.073868	2	1.234	0.751	yes
Apigenin	0.391388	1.2462	1.140723	3	4.332	0.242	yes
ThioTEPA	0.674035	0.937259	0.886101	4	4.357	0.239	yes
Purvalanol	1.673927	2.946799	0.993169	5	0.310	0.959	yes
Oxaliplatin	0.940841	1.226592	0.912785	6	6.314	0.108	yes
β-lapachone	1.670123	3.286734	0.812481	7	5.643	0.143	yes
Topotecan	0.767481	0.689949	1.05592	8	27.112	2.24E-05	yes
Irinotecan	0.793319	0.6301	1.053555	8	29.097	1.03E-05	yes
MG-132	1.109934	1.844122	1.005566	9	15.206	0.0027	yes
ALLN	1.131745	1.887931	1.036945	9	13.149	0.0064	yes
Anisomycin	0.218229	0.875206	0.718368	10	27.492	1.93E-05	yes
Emetin	0.157169	0.781786	0.668568	10	42.104	7.75E-08	yes
Puromycin	0.123195	0.958235	0.69852	10	28.856	1.13E-05	yes

Supplementary Table 8. Identification of unknowns in parallel replicates using BT549 cells. The fluorescence responses ($log_2(I / I_0)$) for each drug were analyzed by LDA specifying the drug identities that are listed on top of the table (from known literature reported mechanisms). Using the shortest Mahalanobis distance of a case from the centroid of the reference groups, *p*-values were calculated. A threshold *p*-value of 0.01 determined if a test case was adjacent to a reference group. A *p*-value <0.01 was considered to be indicative of "novel" mechanism.

Identities: 1 = disruption of mitosis; 2 = topoisomerase II inhibition; 3 = DNA alkylation; 4 = CDK inhibition; 5 = DNA crosslinking; 6 = HDAC inhibition; 7 = necrosis; 8 = topoisomerase I inhibition; 9 = protein degradation; 10 = protein synthesis inhibition; where 8, 9, and 10 are the "novel" mechanistic groups.

Drug name	$log_2(I / I_0)$			Identity	Shortest Mahalanobis distance	*p*-value	Correct prediction
	EBFP2	EGFP	tdTomato				
Paclitaxel	0.491266	1.796443	0.887812	1	7.1	0.076	yes
Paclitaxel	0.365477	1.808655	0.864452	1	6.2	0.111	yes
Paclitaxel	0.385263	1.814733	0.875243	1	7.1	0.076	yes
Paclitaxel	0.446601	1.875363	0.865041	1	6.1	0.116	yes
Paclitaxel	0.461191	1.946412	0.902585	1	12.7	0.007	No
Paclitaxel	0.533706	1.894256	0.889528	1	9.2	0.031	yes
Paclitaxel	0.546818	1.910837	0.900947	1	11.3	0.013	yes
Paclitaxel	0.565304	1.748704	0.900357	1	7.1	0.034	yes
Apigenin	0.331619	1.304964	1.114602	2	5.6	0.143	yes
Apigenin	0.420706	1.137604	1.119796	2	2.9	0.418	yes
Apigenin	0.44792	1.224268	1.135376	2	5	0.182	yes
Apigenin	0.24857	1.297823	1.155536	2	7.1	0.076	yes
Apigenin	0.419364	1.18311	1.118026	2	3.6	0.319	yes
Apigenin	0.446214	1.086631	1.164061	2	4.2	0.252	yes
Apigenin	0.415121	1.353842	1.153021	2	8.1	0.050	yes
Apigenin	0.401591	1.381358	1.165363	2	9.4	0.029	yes
ThioTEPA	0.649454	1.005823	0.915013	3	5	0.182	yes
ThioTEPA	0.603823	0.870318	0.872034	3	2.6	0.467	yes

ThioTEPA	0.566806	0.823415	0.849746	3	3.3	0.358	yes
ThioTEPA	0.71292	0.806894	0.870152	3	4.5	0.223	yes
ThioTEPA	0.700991	1.071011	0.878436	3	9.5	0.028	yes
ThioTEPA	0.748941	1.027028	0.887212	3	9.1	0.033	yes
ThioTEPA	0.789018	1.047493	0.895043	3	10.1	0.021	yes
ThioTEPA	0.620324	0.846092	0.921176	3	1.7	0.644	yes
Purvalanol	1.354938	2.745812	0.891462	4	18.1	0.001	No
Purvalanol	1.450802	2.70905	0.950166	4	6.8	0.087	yes
Purvalanol	1.918678	3.278762	0.964999	4	17.9	0.001	No
Purvalanol	1.812079	3.216549	1.069302	4	8.2	0.048	yes
Purvalanol	1.766307	3.23665	1.069197	4	7.9	0.003	yes
Purvalanol	1.87143	2.983716	1.026729	4	5.2	0.168	yes
Purvalanol	1.681123	2.566447	0.945587	4	8.1	0.050	yes
Purvalanol	1.536059	2.837409	1.027907	4	3.1	0.387	yes
Oxalipatin	0.924969	1.039064	0.872682	5	15	0.003	No
Oxalipatin	0.790845	1.278069	0.904713	5	8.3	0.046	yes
Oxalipatin	0.947535	1.082546	0.90256	5	8.9	0.036	yes
Oxalipatin	0.90064	1.380151	0.92738	5	5.2	0.168	yes
Oxalipatin	0.947591	1.209854	0.914206	5	6.2	0.111	yes
Oxalipatin	0.976698	1.303735	0.92633	5	5.2	0.168	yes
Oxalipatin	1.043034	1.273233	0.912292	5	9.4	0.029	yes
Oxalipatin	0.995412	1.246088	0.942118	5	3.4	0.345	yes
Scriptaid	1.318086	2.168859	1.084297	6	4	0.273	yes
Scriptaid	1.29949	2.300914	1.097074	6	3.5	0.332	yes
Scriptaid	1.232715	2.247992	1.052134	6	1.6	0.666	yes
Scriptaid	1.233967	2.150199	1.049749	6	2.9	0.418	yes
Scriptaid	1.358495	2.028866	1.058505	6	6.3	0.107	yes
Scriptaid	1.341109	2.454851	1.097044	6	2.7	0.450	yes
Scriptaid	1.439778	2.486418	1.086913	6	2.9	0.418	yes
Scriptaid	1.350604	2.522249	1.065231	6	1.3	0.735	yes
β-lapachone	1.635475	3.383322	0.792885	7	3.5	0.332	yes
β-lapachone	1.688223	3.315771	0.856787	7	12	0.010	No

β-lapachone	1.735551	3.367408	0.835724	7	10.6	0.017	yes
β-lapachone	1.81585	3.404662	0.801989	7	12.9	0.007	No
β-lapachone	1.794584	3.359697	0.826125	7	12.8	0.007	No
β-lapachone	1.593027	3.178195	0.784549	7	2.3	0.522	yes
β-lapachone	1.602053	3.275111	0.789168	7	2.1	0.560	yes
β-lapachone	1.496224	3.009709	0.812623	7	7.1	0.076	yes
Topotecan	0.9124558	0.576372	1.0719014	8	34.55	8.12E-07	yes
Topotecan	0.7450821	0.753095	1.0313165	8	19.71	0.0003	yes
Topotecan	0.7804058	0.662567	1.0470668	8	26.11	2.5E-05	yes
Topotecan	0.744172	0.711525	1.0671398	8	29.46	6.32E-06	yes
Topotecan	0.6908895	0.80616	1.0702224	8	25.79	2.86E-05	yes
Topotecan	0.7709816	0.713901	1.0576847	8	25.98	2.64E-05	yes
Topotecan	0.7775269	0.723867	1.058921	8	25.43	3.31E-05	yes
Topotecan	0.7183373	0.572104	1.0431048	8	25.51	3.2E-05	yes
Irinotecan	0.9111066	0.626794	1.0873711	8	34.78	7.39E-07	yes
Irinotecan	0.8906265	0.599745	1.0422428	8	27.15	1.63E-05	yes
Irinotecan	0.6956894	0.514066	1.0048161	8	16.48	0.001	yes
Irinotecan	0.9017144	0.612873	1.0581076	8	29.10	7.33E-06	yes
Irinotecan	0.736761	0.681736	1.0498032	8	25.60	3.08E-05	yes
Irinotecan	0.7294804	0.654143	1.0803982	8	32.83	1.62E-06	yes
Irinotecan	0.7196964	0.697728	1.0441147	8	23.40	7.7E-05	yes
Irinotecan	0.7614738	0.653716	1.0615859	8	30.32	4.46E-06	yes
MG-132	1.1203962	1.820018	1.0453932	9	16.48	0.001	yes
MG-132	1.1054221	1.92109	0.9707078	9	14.16	0.003804	yes
MG-132	1.1020249	1.780509	0.9932195	9	14.50	0.003291	yes
MG-132	1.0754434	1.707923	0.9966842	9	10.43	0.018	No
MG-132	1.0027647	1.810005	0.9880495	9	14.26	0.003644	yes
MG-132	1.1234936	1.904117	1.0037248	9	12.33	0.008294	yes
MG-132	1.2186177	1.869946	1.0275463	9	11.51	0.012	No
MG-132	1.1313061	1.939365	1.0192029	9	10.66	0.017	No
ALLN	0.9805836	1.919773	1.0380716	9	20.00	0.0003	yes
ALLN	1.1916907	1.948941	1.0400151	9	9.10	0.032838	No

ALLN	1.1731707	1.933821	1.0179614	9	9.66	0.025899	No
ALLN	1.1806511	2.009072	1.0121344	9	7.06	0.077671	No
ALLN	1.0311233	1.978185	1.0517562	9	15.86	0.002	yes
ALLN	1.2060096	1.832213	1.0392453	9	13.83	0.004	yes
ALLN	1.1914517	1.724505	1.0420311	9	15.07	0.002	yes
ALLN	1.0992816	1.756937	1.0543426	9	13.80	0.004	yes
Anisomycin	0.2516905	0.823636	0.6897139	10	33.88	1.06E-06	yes
Anisomycin	0.1605141	0.886086	0.7305949	10	27.65	1.32E-05	yes
Anisomycin	0.2931441	0.648547	0.6834973	10	45.36	1.19E-08	yes
Anisomycin	0.1349607	0.882177	0.7263028	10	29.28	6.8E-06	yes
Anisomycin	0.2401371	0.853572	0.7160096	10	28.56	9.12E-06	yes
Anisomycin	0.2457637	0.915057	0.7403855	10	22.74	0.0001	yes
Anisomycin	0.2314582	0.767047	0.6913808	10	37.46	2.56E-07	yes
Anisomycin	0.1881663	1.225528	0.7690587	10	10.60	0.017	No
Emetin	0.1784104	1.330532	0.6540466	10	25.65	3.03E-05	yes
Emetin	0.0967148	0.552381	0.6209228	10	71.12	1.02E-12	yes
Emetin	0.1044868	0.744275	0.7090767	10	40.70	7.17E-08	yes
Emetin	0.2097871	0.68772	0.681943	10	44.83	1.45E-08	yes
Emetin	0.1624354	0.85505	0.6907236	10	33.77	1.11E-06	yes
Emetin	0.1455794	0.383553	0.6822119	10	51.24	1.28E-09	yes
Emetin	0.1858976	0.42808	0.6381867	10	66.97	4.32E-12	yes
Emetin	0.1740443	1.272699	0.6714334	10	22.14	0.0001	yes
Puromycin	0.1751438	0.848196	0.7471039	10	28.46	9.52E-06	yes
Puromycin	0.0208932	0.744188	0.6800961	10	48.82	3.18E-09	yes
Puromycin	0.2036239	0.892739	0.7204562	10	26.66	1.99E-05	yes
Puromycin	0.1489318	0.887767	0.6735382	10	35.39	5.8E-07	yes
Puromycin	0.0722521	1.200062	0.7097523	10	21.76	0.0001	yes
Puromycin	0.1730335	1.083246	0.7083117	10	20.33	0.0002	yes
Puromycin	0.0287076	0.697801	0.7081547	10	48.28	3.9E-09	yes
Puromycin	0.1629762	1.311882	0.6407462	10	30.03	5.01E-06	yes

Supplementary Table 9. Classification of drug combinations using *F*-distribution. The fluorescence responses ($\log_2(I / I_0)$) from the parallel replicates for each drug (using BT549 cells) were analyzed by LDA. The *p*-values were calculated using the shortest Mahalanobis distance of a case from the centroid of the reference mechanisms to which the single drug components of a combination belong to. A threshold *p*-value of 0.01 determined if a test case was adjacent to a single-drug reference mechanism (I, II, and III as defined below). A *p*-value <0.01 was considered to be indicative of "novel" mechanism.

Mechanisms: I = DNA crosslinking; II = Topo II inhibition; III = protein synthesis inhibition; IV = novel.

Drugs included in the reference set: I – cisplatin, oxaliplatin, and chlorambucil; II – daunorubicin, etoposide, doxorubicin, and apigenin; III – anisomycin, emetin, and puromycin (Note: including 4 drugs in the Topo II inihibition mechanism group had the same outcome as using 3 drugs)

Drug name	$\log_2(I / I_0)$			Shortest Mahalanobis distance	*p*-value	Closest mechanism (cut-off $p = 0.01$)
	EBFP2	EGFP	tdTomato			
APG-CSP(1:3)	0.955424	1.106008	1.065095	8.328646	0.047357	I
APG-CSP(1:3)	0.973441	1.146331	1.024337	3.079249	0.393766	I
APG-CSP(1:3)	0.958712	1.206851	1.068932	7.747769	0.060277	I
APG-CSP(1:3)	1.086559	1.295259	1.078068	9.934439	0.024243	I
APG-CSP(1:3)	1.010819	1.272161	1.057487	5.804262	0.134095	I
APG-CSP(1:3)	1.08917	1.315773	1.082389	10.49058	0.019215	I
APG-CSP(1:3)	1.043034	1.304583	1.081454	9.247516	0.032295	I
APG-CSP(1:3)	1.09638	1.359673	1.07246	9.221532	0.032647	I
APG-CSP(3:1)	1.019645	1.367773	1.059276	5.798637	0.134402	I
APG-CSP(3:1)	1.120779	1.481068	1.036317	6.94939	0.083857	I
APG-CSP(3:1)	1.124744	1.524248	1.032358	7.158451	0.076926	I
APG-CSP(3:1)	1.122181	1.525788	1.059937	9.07756	0.034668	I
APG-CSP(3:1)	1.131429	1.557854	1.118681	17.34528	0.001106	IV
APG-CSP(3:1)	1.238708	1.661483	1.056737	17.3487	0.001104	IV
APG-CSP(3:1)	1.175445	1.606648	1.116401	19.24833	0.000505	IV
APG-CSP(3:1)	1.133266	1.764256	1.097466	16.0868	0.001862	IV

PUR-CSP(1:1)	-0.08615	1.622911	0.888862	50.80128	2.91E-09	IV
PUR-CSP(1:1)	0.045809	1.085335	0.824777	15.86019	0.002045	IV
PUR-CSP(1:1)	0.282299	0.933211	0.849196	15.8895	0.002021	IV
PUR-CSP(1:1)	0.248663	1.370993	0.856552	18.06363	0.000822	IV
PUR-CSP(1:1)	0.295679	1.064149	0.845494	14.82667	0.003143	IV
PUR-CSP(1:1)	0.246915	0.939114	0.86624	18.94159	0.000573	IV
PUR-CSP(1:1)	0.367902	1.21823	0.877871	23.49026	8.99E-05	IV
PUR-CSP(1:1)	0.313811	1.178281	0.87533	21.08848	0.000238	IV
PUR-CSP(1:3)	0.132131	0.81462	0.816707	11.42469	0.013002	III
PUR-CSP(1:3)	0.173898	0.822729	0.784728	5.812084	0.133668	III
PUR-CSP(1:3)	0.12376	0.854606	0.813764	10.79458	0.016921	III
PUR-CSP(1:3)	0.158445	0.882777	0.782024	5.256716	0.167431	III
PUR-CSP(1:3)	0.188832	1.110528	0.847513	14.76294	0.003227	IV
PUR-CSP(1:3)	0.198981	0.889976	0.854416	16.8847	0.001338	IV
PUR-CSP(1:3)	0.222699	1.165705	0.84713	14.54853	0.003529	IV
PUR-CSP(1:3)	0.245328	0.982695	0.788376	5.695164	0.140181	III
PUR-APG(1:1)	0.729879	0.973113	0.675937	53.83391	1E-09	IV
PUR-APG(1:1)	0.812728	1.22745	0.674566	55.89781	4.89E-10	IV
PUR-APG(1:1)	0.591799	0.892395	0.703146	30.84083	4.87E-06	IV
PUR-APG(1:1)	1.015348	0.891376	0.659702	64.25754	2.87E-11	IV
PUR-APG(1:1)	0.712939	0.860641	0.740408	34.52504	1.17E-06	IV
PUR-APG(1:1)	0.665525	1.118378	0.774402	30.29744	6.02E-06	IV
PUR-APG(1:1)	0.796373	1.293681	0.753162	31.54274	3.71E-06	IV
PUR-APG(1:1)	0.644193	1.19995	0.729385	37.98025	3.15E-07	IV
PUR-APG(3:1)	0.352239	0.718765	0.62538	11.31612	0.013606	III
PUR-APG(3:1)	0.523196	0.829024	0.659261	24.7313	5.46E-05	IV
PUR-APG(3:1)	0.448536	0.865448	0.614883	21.09229	0.000238	IV
PUR-APG(3:1)	0.516575	0.620904	0.595459	33.79111	1.55E-06	IV
PUR-APG(3:1)	0.370689	0.636177	0.669956	10.03931	0.023203	III
PUR-APG(3:1)	0.538742	0.500122	0.637354	33.15634	1.98E-06	IV
PUR-APG(3:1)	0.501424	0.751816	0.661113	22.37575	0.000141	IV
PUR-APG(3:1)	0.47177	0.754987	0.639533	20.88916	0.000258	IV

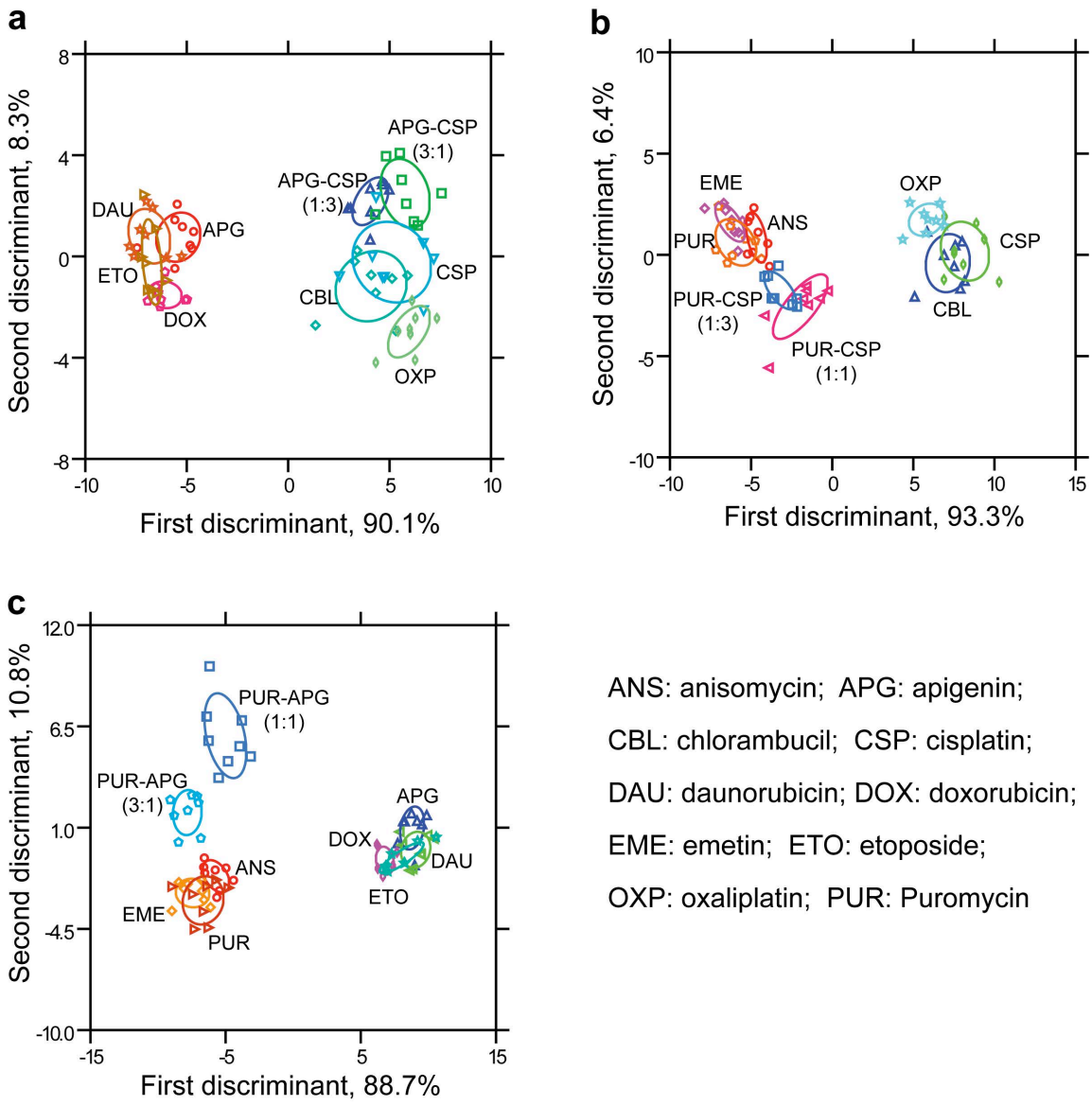

Supplementary Figure 13. Categorizing the mechanisms of drug combinations. BT549 Cells were treated with the drug combinations for 24 h at their corresponding IC_{50} concentrations. Canonical score plot of the synergistic combinations of **b,** apigenin-cisplatin, **c,** puromycin-cisplatin, and **d,** puromycin-apigenin were derived from LDA of the fluorescence responses and plotted with 95% confidence ellipses around the centroid of each group. The identities of individual drugs from the mechanistic groups, to which the drug components of the combinations belong to, were retained in the LDA analysis.

Section 6: Discussions on the Importance of the Fluorescence Channels

It is worth examining the importance of the individual FP in the multi-channel sensor. We drug categorized the drugs as well as identified the unknowns using to investigate whether or not different FP pairs provide equivalent or better classification resolution than the triple-channel.

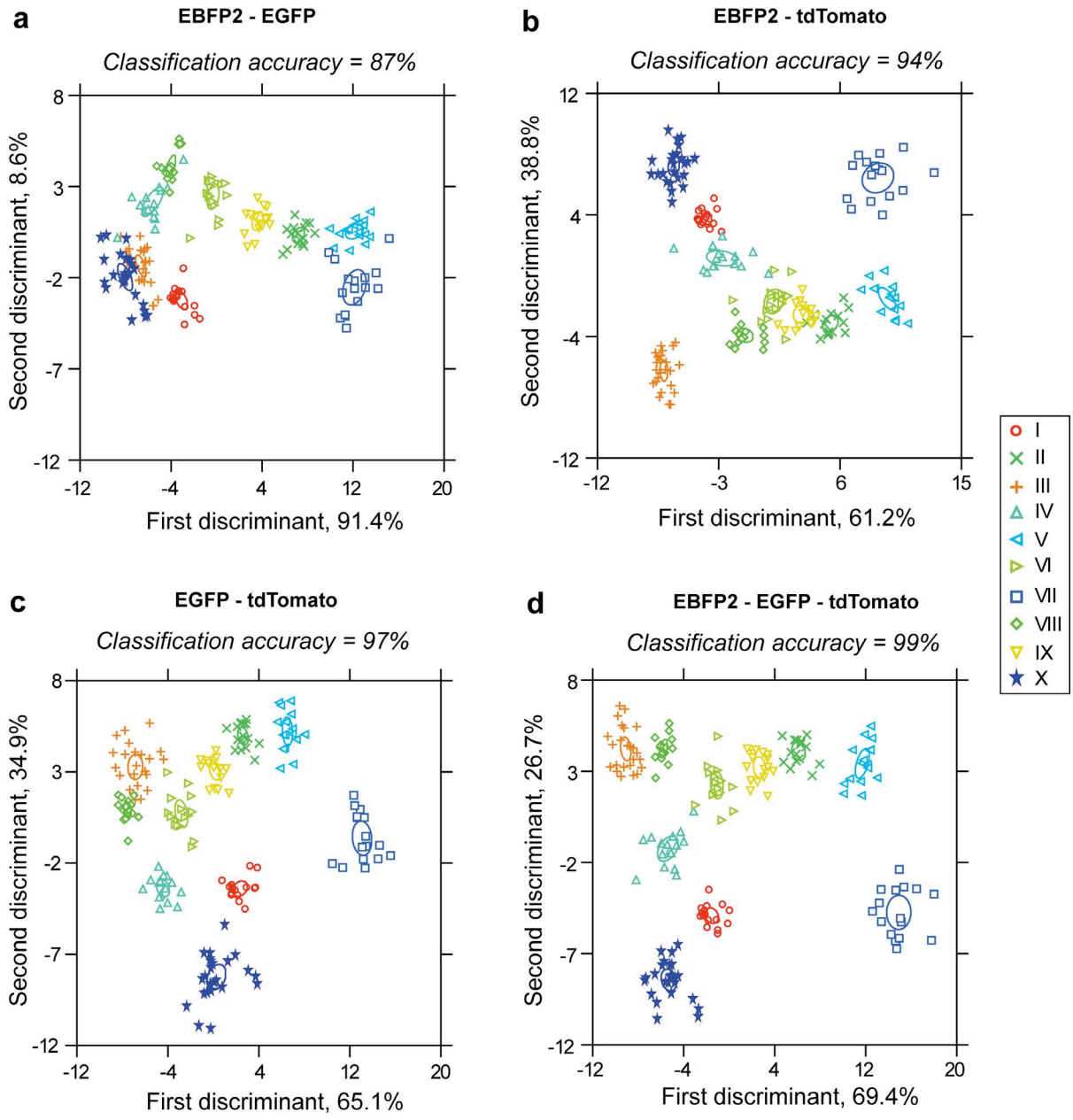

Supplementary Figure 14. Significance of the FPs in categorizing the drug mechanisms using BT549 cells. The canonical score plots were derived from LDA of the fluorescence responses

obtained from the FP combinations of **a**, EBFP2-EGFP, **b**, EBFP2-tdtomato, **c**, EGFP-tdTomato, and **d**, EBFP2-EGFP-tdTomato, and plotted with 95% confidence ellipses around the centroid of each group (based on the standard error of the mean). The Jackknifed classification accuracy is noted on the top of each plot. Identities: I= disruption of mitosis (vinblastine sulfate, vincristine sulfate); II= HDAC inhibition (apicidin, vorinostat); III= topoisomerase II inhibition (daunorubicin HCl, etoposide, doxorubicin HCl); IV= DNA alkylation (6-thioguanine, temozolomide); V= CDK inhibition (roscovitine, olomoucine); VI= DNA crosslinking (cisplatin, chlorambucil); VII= necrosis (sodium nitroprusside, hydrogen peroxide); VIII= topoisomerase I inhibition (topotecan, irniotecan); IX= protein degradation (MG-132, ALLN); X= protein synthesis inhibition (anisomycin, emetin, puromycin).

Apparently, the responses for tdTomato in the triple-channel sensor seem to vary slightly across the drug set (Fig. 3a and Supplementary Fig. 10). However, a systematic analysis of the fluorescence responses with and without tdTomato (Supplementary Fig. 14) demonstrates that this FP provides a significant contribution towards the overall categorization. Interestingly, tdTomato in combination with EGFP provided much higher classification accuracy (Jackknifed) than the EBFP2-EGFP pair (97% *vs*. 87%). Also, it is evident that the triple-channel combination categorized the reference set with the greatest classification accuracy. The high classification accuracy of the EGFP-tdTomato pair prompted us to further compare its ability to identify the blinded unknowns and 'novel' categories with the triple-channel combination (Supplementary Fig. 15 and Supplementary Table 10).

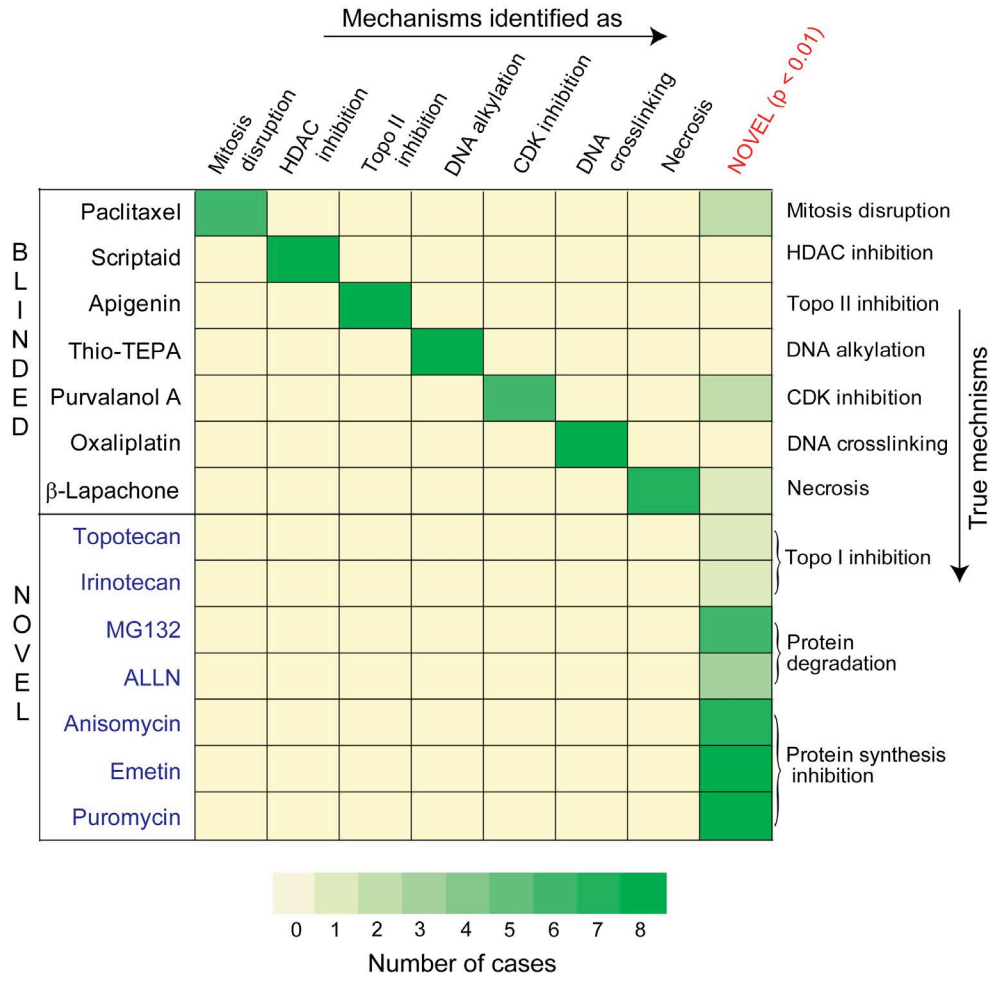

Supplementary Figure 15. Prediction of drug mechanisms on parallel replicates using fluorescence responses from EGFP-tdTomato pair. Fluorescence responses only from the EGFP, and tdTomato channels were utilized to perform the statistical analysis. The *p*-values were derived from *F*-distribution on the minimum Mahalanobis distance (derived from LDA) of each replicate to the centroid of reference groups. Based on the *p*-values, each unknown case (parallel replicate) was assigned to a reference mechanistic group or regarded as 'novel'. The blinded unknowns exhibits cell death mechanisms similar to the reference set, while the 'novel' unknowns involve mechanisms completely different from the reference set.

Supplementary Table 10. Identification of unknowns using the EGFP-tdTomato channels only (BT549 cells). The average fluorescence responses ($log_2(I / I_0)$) of eight replicates for each drug was analyzed by LDA specifying the drug identities that are listed on top of the table (from known literature reported mechanisms). A threshold *p*-value of 0.01 determined if test case was adjacent to a reference group or indicative of "novel" mechanism. **Compare table 7.**

Identities: 1 = disruption of mitosis; 2 = HDAC inhibition; 3 = topoisomerase II inhibition; 4 = DNA alkylation; 5 = CDK inhibition; 6 = DNA crosslinking; 7 = necrosis; 8 = topoisomerase I inhibition; 9 = protein degradation; 10 = protein synthesis inhibition; where 8, 9, and 10 are the "novel" mechanistic groups.

Drug name	$log_2(I / I_0)$		Identity	Shortest Mahalanobis distance	*p*-value	Correct prediction
	EGFP	tdTomato				
Paclitaxel	1.849425	0.885746	1	7.66	0.024	yes
Scriptaid	2.295043	1.073868	2	1.22	0.548	yes
Apigenin	1.2462	1.140723	3	3.91	0.147	yes
ThioTEPA	0.937259	0.886101	4	3.11	0.217	yes
Purvalanol	2.946799	0.993169	5	0.25	0.881	yes
Oxaliplatin	1.226592	0.912785	6	5.82	0.058	yes
β-lapachone	3.286734	0.812481	7	3.14	0.214	yes
Topotecan	0.689949	1.05592	8	5.49	0.068	no
Irinotecan	0.6301	1.053555	8	7.13	0.031	no
MG-132	1.844122	1.005566	9	12.66	0.002	yes
ALLN	1.887931	1.036945	9	10.51	0.06	no
Anisomycin	0.875206	0.718368	10	26.32	5.3E-06	yes
Emetin	0.781786	0.668568	10	40.39	1.5E-08	yes
Puromycin	0.958235	0.69852	10	24.67	1.1E-05	yes

Taken together, it can be inferred with confidence that all the three FPs are crucial to achieve the highest accuracy of classifying the reference set as well as identifying the unknowns.

In fact, tdTomato with seemingly less variant fluorescence responses provides great contribution towards the classification ability of the triple-channel sensor.

Section 7: Supplementary Data

Supplementary Table 11. Raw fluorescence responses and LDA output data set for the chemotherapeutic-treated BT549 cells. Score (1), score (2), and score (3) are generated along the first, second, and third discriminants, respectively (corresponding to Fig. 3b).

Drug name	$\log_2(I / I_0)$			LDA output		
	EBFP2	EGFP	tdTomato	Score (1)	Score (2)	Score (3)
Vinblastin	0.46029	1.81061	0.83199	-0.33733	-5.18269	-2.95159
Vinblastin	0.380047	1.517309	0.810265	-1.87681	-6.26215	-2.00207
Vinblastin	0.428491	1.663509	0.802253	-0.6889	-6.26144	-2.26736
Vinblastin	0.371378	1.464595	0.809039	-2.16985	-6.35679	-1.80236
Vinblastin	0.440235	1.505213	0.821917	-1.7885	-5.72053	-1.51858
Vinblastin	0.398748	1.470653	0.821442	-2.21073	-5.89095	-1.69193
Vinblastin	0.411077	1.522519	0.799521	-1.44724	-6.47912	-1.68849
Vinblastin	0.409194	1.499347	0.817092	-1.91749	-5.97106	-1.71592
Vincristine	0.47884	1.887598	0.821312	0.370812	-5.39908	-3.10309
Vincristine	0.458132	1.541584	0.769926	-0.48051	-7.20105	-1.17227
Vincristine	0.425527	1.452845	0.806867	-1.84769	-6.24968	-1.27114
Vincristine	0.370902	1.767977	0.792272	-0.3331	-6.69309	-3.20355
Vincristine	0.487601	1.754317	0.792028	0.332718	-6.32262	-2.14931
Vincristine	0.382557	1.490518	0.813859	-2.06484	-6.16091	-1.87287
Vincristine	0.387964	1.51053	0.788098	-1.42845	-6.90481	-1.74043
Vincristine	0.537889	1.414379	0.839616	-1.97665	-4.91747	-0.36883
Daunorubicin	0.290611	1.342452	1.166512	-10.2611	4.033232	-4.4673
Daunorubicin	0.237986	1.031847	1.136932	-11.5609	2.79973	-3.14123
Daunorubicin	0.388378	0.912308	1.10361	-10.5668	2.230349	-1.03263
Daunorubicin	0.253959	0.730424	1.133694	-12.9006	2.588111	-1.47392
Daunorubicin	0.335802	0.980681	1.114151	-10.7602	2.410888	-1.89482

Daunorubicin	0.381056	0.774999	1.159992	-12.3976	3.821506	-0.81627
Daunorubicin	0.298169	1.005882	1.157684	-11.7194	3.606631	-2.65441
Daunorubicin	0.359246	1.02196	1.182147	-11.7352	4.551149	-2.39747
Etoposide	0.263882	1.092634	1.126215	-10.8869	2.597442	-3.14939
Etoposide	0.266421	0.582569	1.071296	-12.3419	0.675232	-0.17555
Etoposide	0.241704	0.78753	1.083549	-11.7137	1.074914	-1.4991
Etoposide	0.275676	0.741085	1.116499	-12.3761	2.14986	-1.21932
Etoposide	0.25879	0.897028	1.081166	-11.0145	1.120591	-1.88593
Etoposide	0.300674	1.053831	1.095843	-10.2576	1.786211	-2.42435
Etoposide	0.35388	0.90617	1.144354	-11.6082	3.335384	-1.58862
Etoposide	0.369534	0.900618	1.183357	-12.2994	4.55412	-1.712
Doxorubicin	0.301946	1.167641	1.110823	-9.97471	2.30297	-3.09219
Doxorubicin	0.252626	0.797817	1.061572	-11.1652	0.457361	-1.29893
Doxorubicin	0.222929	0.806211	1.074457	-11.5604	0.75054	-1.68494
Doxorubicin	0.341384	0.867091	1.056599	-10.1682	0.639718	-0.86121
Doxorubicin	0.244624	1.332412	1.109955	-9.49449	2.179048	-4.3942
Doxorubicin	0.240686	1.327656	1.094736	-9.24574	1.706824	-4.2931
Doxorubicin	0.329514	0.987095	1.063413	-9.77711	0.871492	-1.61158
Doxorubicin	0.256307	1.054607	1.089364	-10.4045	1.445764	-2.75533
Temozolomide	0.24285	0.553495	0.863899	-8.58582	-5.6408	1.27703
Temozolomide	0.453463	0.451371	0.913575	-8.74864	-3.51167	3.203663
Temozolomide	0.644015	0.70445	0.890903	-5.85385	-3.42219	3.708041
Temozolomide	0.491118	0.880961	0.867413	-5.4707	-4.5339	1.70556
Temozolomide	0.56293	0.716296	0.890127	-6.28627	-3.70666	2.970621
Temozolomide	0.524007	0.818792	0.892328	-6.06144	-3.71232	2.113265
Temozolomide	0.520839	0.79449	0.907881	-6.50598	-3.26965	2.0953
Temozolomide	0.874005	0.743587	0.932008	-5.02408	-1.40781	5.153067
6-Thioguanine	0.753964	0.630333	0.884803	-5.4173	-3.28323	5.050558
6-Thioguanine	0.534404	0.599958	0.88291	-6.9036	-4.08193	3.364929
6-Thioguanine	0.490049	0.670069	0.865123	-6.48403	-4.72313	2.769025
6-Thioguanine	0.542452	0.765211	0.847565	-5.33957	-5.02405	2.862058
6-Thioguanine	0.646323	0.66954	0.906376	-6.31548	-2.96973	3.789952
6-Thioguanine	0.693022	0.757648	0.912566	-5.70529	-2.58093	3.697676
6-Thioguanine	0.47827	0.585993	0.919337	-8.035	-3.18219	2.697015

6-Thioguanine	0.511263	0.6918	0.907708	-7.07437	-3.36344	2.529933
Roscovitine	1.481512	2.791375	0.981246	8.019372	3.211492	-0.33403
Roscovitine	1.520088	2.635046	0.954074	8.011433	2.43697	0.97122
Roscovitine	1.611893	2.807801	0.946511	9.5939	2.609078	0.935368
Roscovitine	1.745599	2.928981	1.020856	9.582234	5.348257	0.916368
Roscovitine	1.71224	3.029648	1.027333	9.749245	5.488238	0.084046
Roscovitine	1.812353	2.943817	1.05868	9.33499	6.711663	1.130383
Roscovitine	1.62934	2.831877	1.029942	8.194416	5.183043	0.356211
Roscovitine	1.730372	3.087695	1.048841	9.732078	6.225598	-0.20983
Olomoucine	1.673132	2.858371	1.001484	9.155582	4.488599	0.799449
Olomoucine	1.56894	2.967676	0.981787	9.433964	3.614257	-0.48339
Olomoucine	1.673112	2.973207	1.002772	9.702812	4.590871	0.215005
Olomoucine	1.680373	2.948203	0.99496	9.776022	4.366605	0.458137
Olomoucine	1.681203	3.088029	0.980645	10.75768	4.017468	-0.131
Olomoucine	1.728634	2.953381	1.052093	8.988169	6.242891	0.424364
Olomoucine	1.705593	2.833042	1.003425	9.194247	4.639975	1.185906
Olomoucine	1.561515	2.763998	0.981421	8.379332	3.465753	0.476394
Cisplatin	0.955463	1.120609	1.005457	-4.06924	1.273854	3.419105
Cisplatin	0.91456	1.335061	0.979145	-2.74212	0.468383	2.191539
Cisplatin	1.021664	1.278595	0.932405	-1.44208	-0.6115	3.716759
Cisplatin	0.95197	1.187528	0.982773	-3.31468	0.618903	3.21931
Cisplatin	1.046955	1.310746	1.069862	-3.80685	3.613667	2.771069
Cisplatin	0.960188	1.143872	0.979884	-3.42458	0.535148	3.528148
Cisplatin	0.897941	1.470034	1.006944	-2.7157	1.322379	1.173817
Cisplatin	0.987482	1.133257	0.996451	-3.63035	1.116436	3.691162
Chlorambucil	0.915784	1.293391	0.997033	-3.29137	0.985958	2.280613
Chlorambucil	0.907607	1.187538	0.972061	-3.38272	0.151038	2.922937
Chlorambucil	0.909298	1.230225	0.926123	-2.26268	-1.19786	3.057004
Chlorambucil	1.019955	1.401118	0.981318	-1.79671	0.918265	2.733796
Chlorambucil	0.671492	1.292735	0.980329	-4.49496	-0.32225	0.34517
Chlorambucil	0.979797	1.167068	0.975416	-3.09922	0.47874	3.609803
Chlorambucil	0.876173	1.498585	1.029895	-3.15737	1.954885	0.680678
Chlorambucil	0.913574	1.228439	1.025322	-4.18117	1.791327	2.381781
Apicidin	1.286911	2.408918	1.036151	3.82511	4.00392	-0.45884

Apicidin	1.358421	2.202612	1.031102	3.341972	3.974146	1.213719
Apicidin	1.419501	2.515991	1.015953	5.581591	3.895202	0.269808
Apicidin	1.420256	2.401426	1.066837	4.021933	5.360708	0.480312
Apicidin	1.377233	2.381202	0.994637	5.061612	3.041342	0.742974
Apicidin	1.399874	2.363998	1.045443	4.1256	4.630792	0.65116
Apicidin	1.314384	2.482715	1.067468	3.75337	5.075125	-0.82401
Apicidin	1.267388	2.210915	1.074821	1.961208	4.989752	0.087086
Vorinostat	1.335615	2.429201	1.062762	3.711098	4.974364	-0.34289
Vorinostat	1.165903	2.322986	1.039631	2.57271	3.661068	-1.07429
Vorinostat	1.27831	2.2844	1.044964	2.978595	4.170837	0.028058
Vorinostat	1.206381	2.338187	1.023428	3.217675	3.317066	-0.69142
Vorinostat	1.312167	2.271006	1.02524	3.508365	3.683462	0.52382
Vorinostat	1.315973	2.343126	1.066188	3.092412	4.964513	-0.10245
Vorinostat	1.311374	2.407644	1.068408	3.341969	5.051724	-0.48038
Vorinostat	1.313587	2.456546	1.061648	3.731532	4.88337	-0.65747
Hydrogen peroxide	1.620219	3.488785	0.697291	18.14489	-1.76265	-1.9612
Hydrogen peroxide	1.312069	3.411004	0.725453	16.34856	0.109502	-0.86531
Hydrogen peroxide	1.481707	3.251791	0.73834	17.7015	-0.34352	-0.58014
Hydrogen peroxide	1.504301	3.201843	0.741305	19.2286	-1.09804	0.536763
Hydrogen peroxide	1.397866	3.154278	0.721031	18.03658	-0.5116	0.54902
Hydrogen peroxide	1.473657	3.131516	0.705418	15.1054	-2.36669	-0.11895
Hydrogen peroxide	1.441867	2.773747	0.747939	16.42744	-2.08836	-1.11461
Hydrogen peroxide	1.45703	2.873859	0.730249	12.09778	-1.94325	0.037757
Sodium nitroprusside	1.340388	3.327158	0.705639	15.18832	-5.22575	-2.2055
Sodium nitroprusside	1.307178	3.288366	0.792712	13.0878	-2.74466	-2.92352
Sodium nitroprusside	1.576952	3.29071	0.794769	14.74492	-1.79079	-0.6753
Sodium nitroprusside	1.461543	3.362476	0.80259	14.22895	-1.89746	-2.06458
Sodium nitroprusside	1.344505	3.316989	0.814749	13.03358	-1.94438	-2.91206
Sodium nitroprusside	1.841151	3.295679	0.754473	17.20701	-2.12453	1.820263
Sodium nitroprusside	1.549163	3.356486	0.831951	14.17343	-0.73058	-1.50891
Sodium nitroprusside	1.657052	3.372415	0.785417	15.83527	-1.76155	-0.34101

Supplementary Table 12. Fluorescence responses and LDA output data set for the chemotherapeutic-treated pTD cells. Score (1), score (2), and score (3) are generated along the first, second, and third discriminants, respectively (corresponding to Supplementary Fig. 10b).

Drug name	$\log_2(I / I_0)$			LDA output		
	EBFP2	EGFP	tdTomato	Score (1)	Score (2)	Score (3)
Vinblastin	0.630556	1.957531	1.680709	0.504259	-4.91872	1.688903
Vinblastin	0.401922	1.927864	1.635725	-0.88552	-4.50096	-1.44021
Vinblastin	0.435552	1.695543	1.616662	-3.50084	-3.46025	0.251953
Vinblastin	0.412167	1.729815	1.632945	-3.50084	-3.46025	0.251953
Vinblastin	0.434028	2.043613	1.689536	-3.09337	-4.22442	0.084623
Vinblastin	0.446365	1.723553	1.612482	0.860025	-6.41012	-0.85241
Vinblastin	0.56714	2.04731	1.646829	-3.17556	-3.25813	0.072004
Vinblastin	0.540976	2.086295	1.626352	1.086291	-4.05438	-0.34924
Vincristine	0.886513	2.612557	1.681916	8.739679	-3.89615	-0.44734
Vincristine	0.902607	2.555101	1.689547	8.196373	-4.05917	0.30796
Vincristine	0.78999	2.588394	1.664533	8.032228	-3.77357	-1.64863
Vincristine	0.741848	2.587967	1.644509	7.739072	-3.2921	-2.56823
Vincristine	0.764939	2.459168	1.645238	6.374786	-3.11492	-1.35018
Vincristine	0.718142	2.445098	1.657676	6.135671	-3.83885	-1.48515
Vincristine	0.749986	2.42496	1.639104	5.901396	-2.94893	-1.38054
Vincristine	0.782768	2.422856	1.690048	6.307152	-4.67853	0.032229
Paclitaxel	0.577658	1.998416	1.644243	0.556444	-3.86955	0.072731
Paclitaxel	0.612453	2.026605	1.646813	1.007238	-3.78599	0.284703
Paclitaxel	0.647319	2.012569	1.619186	0.795224	-2.54198	0.189376
Paclitaxel	0.587927	1.970928	1.641409	0.264721	-3.68916	0.327687
Paclitaxel	0.429575	1.936762	1.628178	-0.73889	-4.0661	-1.36887
Paclitaxel	0.548253	1.899939	1.623889	-0.77689	-3.21338	0.074423
Paclitaxel	0.517597	1.930853	1.625483	-0.52357	-3.46428	-0.44761
Paclitaxel	0.436949	1.914318	1.644195	-0.866	-4.61391	-0.7937
Cisplatin	1.124965	2.69522	1.664108	10.366	-1.92747	1.097686
Cisplatin	1.171314	2.707877	1.680162	10.76568	-2.27678	1.825492

Cisplatin	1.238316	2.741382	1.669884	11.3052	-1.53118	2.074476
Cisplatin	1.221971	2.74838	1.649104	11.19859	-0.84601	1.421027
Cisplatin	1.217497	2.748448	1.655691	11.22532	-1.11904	1.508819
Cisplatin	1.176029	2.731926	1.676629	11.02983	-2.13117	1.623738
Cisplatin	1.13752	2.742506	1.646217	10.82813	-1.21099	0.510279
Cisplatin	1.076274	2.713351	1.661412	10.38773	-2.1115	0.39124
Chlorambucil	1.235347	2.766191	1.633633	11.34744	-0.1989	1.111473
Chlorambucil	1.175601	2.733356	1.639049	10.8097	-0.72105	0.834211
Chlorambucil	1.030869	2.661956	1.625798	9.43381	-0.99889	-0.44138
Chlorambucil	1.303803	2.766129	1.665821	11.77998	-1.02284	2.500651
Chlorambucil	0.9696	2.824435	1.624308	11.04228	-1.38249	-2.33026
Chlorambucil	1.323343	2.708493	1.664513	11.1905	-0.83007	3.109586
Chlorambucil	1.102844	2.647764	1.622652	9.498818	-0.46593	0.362142
Chlorambucil	0.989329	2.610561	1.631821	8.753078	-1.43039	-0.3751
Carboplatin	1.063679	2.73337	1.643247	10.45647	-1.51101	-0.26547
Carboplatin	1.190691	2.675835	1.635091	10.18987	-0.45383	1.34055
Carboplatin	1.19318	2.673393	1.603239	9.971919	0.759542	0.728786
Carboplatin	1.262736	2.669629	1.595958	10.12006	1.428331	1.343887
Carboplatin	1.228341	2.61973	1.59369	9.428578	1.348156	1.303916
Carboplatin	1.222154	2.628996	1.616273	9.652765	0.458559	1.63473
Carboplatin	1.199825	2.659926	1.635312	10.04347	-0.4014	1.560267
Carboplatin	1.285613	2.681033	1.60343	10.37246	1.269928	1.655446
Gemcitabin	0.86328	2.11592	1.576631	2.423125	0.218476	0.832212
Gemcitabin	0.79707	1.98594	1.614163	0.972568	-1.49204	1.870975
Gemcitabin	0.686703	1.889941	1.586165	-0.65527	-1.00703	0.838742
Gemcitabin	0.625041	1.99694	1.562156	0.187844	-0.51396	-1.10554
Gemcitabin	0.64547	2.090814	1.592199	1.49953	-1.58257	-0.96846
Gemcitabin	0.741564	1.839227	1.566843	-1.15971	0.058678	1.399327
Gemcitabin	0.730865	2.049459	1.564365	1.150649	-0.02967	-0.32932
Gemcitabin	0.600512	1.949159	1.570936	-0.37737	-0.95514	-0.82906
6-Thioguanine	0.688536	1.965869	1.553561	0.000404	0.185772	-0.37858
6-Thioguanine	0.619743	1.917595	1.545358	-0.82656	0.133622	-0.91747

6-Thioguanine	0.615466	1.908244	1.537634	-0.99438	0.405323	-1.05236
6-Thioguanine	0.509227	1.920736	1.551439	-1.12812	-0.72102	-1.98671
6-Thioguanine	0.618073	1.880192	1.550011	-1.22342	-0.02925	-0.561
6-Thioguanine	0.568824	1.997175	1.530262	-0.19941	0.367951	-2.36023
6-Thioguanine	0.582786	1.873655	1.550389	-1.41419	-0.23899	-0.87851
6-Thioguanine	0.524241	1.848715	1.558608	-1.84164	-0.86434	-1.14403
Doxorubicin	0.297262	1.358871	1.505767	-8.44534	0.123459	-0.99363
Doxorubicin	0.277678	1.430376	1.480565	-7.86577	0.919464	-2.25249
Doxorubicin	0.348069	1.256603	1.501721	-9.44735	0.621476	0.222335
Doxorubicin	0.281748	1.278143	1.491812	-9.49217	0.60717	-0.84494
Doxorubicin	0.361372	1.324882	1.503919	-8.62134	0.574587	-0.09942
Doxorubicin	0.332713	1.409132	1.494201	-7.83262	0.729646	-1.23021
Doxorubicin	0.349506	1.472089	1.502145	-7.01867	0.489455	-1.35699
Doxorubicin	0.314372	1.419098	1.480997	-7.86533	1.116917	-1.77079
Daunorubicin	0.308974	1.477233	1.526707	-6.94493	-0.66615	-1.31869
Daunorubicin	0.32402	1.449659	1.533756	-7.15967	-0.83042	-0.80884
Daunorubicin	0.322749	1.383207	1.534893	-7.90353	-0.84204	-0.30446
Daunorubicin	0.307977	1.39178	1.560813	-7.69541	-1.90521	0.009289
Daunorubicin	0.31671	1.378203	1.53364	-7.98806	-0.82614	-0.35704
Daunorubicin	0.325987	1.508397	1.514276	-6.61472	-0.12051	-1.62642
Daunorubicin	0.308587	1.398851	1.506587	-7.95259	0.133521	-1.15419
Daunorubicin	0.314391	1.365078	1.556076	-8.00326	-1.67547	0.178339
Camptothecin	0.136312	0.652756	1.471979	-17.1361	0.892176	1.858219
Camptothecin	0.274602	0.630702	1.431294	-17.1689	3.215963	2.649517
Camptothecin	0.009483	0.519143	1.47653	-19.039	0.081804	1.602046
Camptothecin	0.267718	0.574035	1.394001	-18.0619	4.612283	2.229763
Camptothecin	-0.02895	0.479855	1.403553	-20.0667	2.631929	-0.01665
Camptothecin	0.149514	0.480191	1.392692	-19.5254	4.048045	1.648379
Camptothecin	0.290864	0.493261	1.418027	-18.7409	3.885956	3.571091
Camptothecin	0.109625	0.449518	1.399135	-19.9651	3.598172	1.586609
Irinotecan	-0.01797	0.454143	1.367814	-20.5415	4.052881	-0.44531
Irinotecan	-0.15665	0.558302	1.449392	-19.332	0.141691	-1.00904

Irinotecan	-0.06199	0.44893	1.392628	-20.5944	2.874087	-0.36174
Irinotecan	-0.13783	0.460991	1.431576	-20.4729	0.974091	-0.45265
Irinotecan	-0.08313	0.560204	1.42537	-19.2114	1.459164	-0.73912
Irinotecan	-0.01824	0.295653	1.521986	-21.3602	-1.65551	3.907726
Irinotecan	-0.3494	0.431042	1.510202	-21.0358	-3.16044	-0.85185
Irinotecan	-0.29223	0.334469	1.459628	-22.2429	-0.87995	-0.56956
Sodium nitroprusside	1.439304	2.661759	1.538715	10.27296	4.582811	2.094137
Sodium nitroprusside	1.425193	2.617447	1.508984	9.541505	5.646792	1.661684
Sodium nitroprusside	1.342859	2.67758	1.55496	10.22507	3.418096	1.289067
Sodium nitroprusside	1.317269	2.588025	1.533766	8.99966	4.122276	1.247499
Sodium nitroprusside	1.256974	2.61168	1.556089	9.200386	2.928583	0.892496
Sodium nitroprusside	1.333782	2.664011	1.511392	9.769687	5.013199	0.396116
Sodium nitroprusside	1.287174	2.679908	1.511017	9.787883	4.754916	-0.2238
Sodium nitroprusside	1.308869	2.64991	1.517661	9.56591	4.644858	0.366204
Hydrogen peroxide	1.280304	2.67307	1.460555	9.372544	6.617892	-1.28552
Hydrogen peroxide	1.161565	2.59995	1.444539	8.048212	6.591827	-2.32981
Hydrogen peroxide	1.247158	2.605825	1.433333	8.334537	7.493246	-1.69737
Hydrogen peroxide	1.202649	2.65799	1.430024	8.749024	7.336279	-2.62536
Hydrogen peroxide	1.406545	2.604326	1.426408	8.815034	8.654625	-0.13979
Hydrogen peroxide	1.313312	2.624207	1.428027	8.732311	8.055769	-1.24238
Hydrogen peroxide	1.194607	2.690205	1.424677	9.050307	7.473393	-3.06044
Hydrogen peroxide	1.271207	2.612001	1.43927	8.522581	7.402212	-1.36613

Supplementary Table 13. Fluorescence response data from drug candidates and their combinations using BT549 cells. Score (1), score (2), and score (3) are generated along the first, second, and third discriminants, respectively (corresponding to Fig. 4b,c,d).

Drug name	$\log_2(I / I_0)$			LDA output		
	EBFP2	EGFP	tdTomato	Score (1)	Score (2)	Score (3)
PUR-APG(1:1)	0.729879	0.973113	0.675937	5.520782	4.907233	-0.12995
PUR-APG(1:1)	0.812728	1.22745	0.674566	5.83439	5.893113	-1.22432
PUR-APG(1:1)	0.591799	0.892395	0.703146	4.596559	3.178478	0.161429

PUR-APG(1:1)	1.015348	0.891376	0.659702	5.94494	8.566886	0.478503
PUR-APG(1:1)	0.712939	0.860641	0.740408	3.42826	4.748557	0.482642
PUR-APG(1:1)	0.665525	1.118378	0.774402	2.656983	4.085279	-0.68531
PUR-APG(1:1)	0.796373	1.293681	0.753162	3.497753	5.697772	-1.40727
PUR-APG(1:1)	0.644193	1.19995	0.729385	4.119737	3.772008	-1.15735
PUR-APG(3:1)	0.352239	0.718765	0.62538	6.782801	0.137884	0.604738
PUR-APG(3:1)	0.523196	0.829024	0.659261	5.869857	2.302778	0.31361
PUR-APG(3:1)	0.448536	0.865448	0.614883	7.263011	1.321742	0.001174
PUR-APG(3:1)	0.516575	0.620904	0.595459	7.603212	2.250475	1.152659
PUR-APG(3:1)	0.370689	0.636177	0.669956	5.332344	0.414483	1.078041
PUR-APG(3:1)	0.538742	0.500122	0.637354	6.194798	2.584081	1.800095
PUR-APG(3:1)	0.501424	0.751816	0.661113	5.730845	2.0472	0.651405
PUR-APG(3:1)	0.47177	0.754987	0.639533	6.393334	1.659093	0.572327
PUR-CSP(1:1)	-0.08615	1.622911	0.888862	-3.94154	-4.88514	2.473551
PUR-CSP(1:1)	0.045809	1.085335	0.824777	-3.78735	-2.61982	0.185421
PUR-CSP(1:1)	0.282299	0.933211	0.849196	-1.43582	-1.59412	-0.77301
PUR-CSP(1:1)	0.248663	1.370993	0.856552	-1.49937	-1.97369	1.420009
PUR-CSP(1:1)	0.295679	1.064149	0.845494	-1.32605	-1.42426	-0.07359
PUR-CSP(1:1)	0.246915	0.939114	0.86624	-1.52189	-2.19937	-0.86808
PUR-CSP(1:1)	0.367902	1.21823	0.877871	-0.21939	-1.65354	0.48021
PUR-CSP(1:1)	0.313811	1.178281	0.87533	-0.74057	-1.95505	0.293397
PUR-CSP(1:3)	0.132131	0.81462	0.816707	-3.21815	-1.87618	-1.14437
PUR-CSP(1:3)	0.173898	0.822729	0.784728	-3.26717	-0.90283	-0.86768
PUR-CSP(1:3)	0.12376	0.854606	0.813764	-3.31787	-1.86689	-0.91756
PUR-CSP(1:3)	0.158445	0.882777	0.782024	-3.4198	-0.94534	-0.5397
PUR-CSP(1:3)	0.188832	1.110528	0.847513	-2.22451	-2.17263	0.148891
PUR-CSP(1:3)	0.198981	0.889976	0.854416	-2.11334	-2.25775	-1.03387
PUR-CSP(1:3)	0.222699	1.165705	0.84713	-1.91468	-1.94059	0.435187
PUR-CSP(1:3)	0.245328	0.982695	0.788376	-2.54183	-0.51037	-0.07279
APG-CSP(1:3)	0.955424	1.106008	1.065095	2.150454	1.22986	1.540538
APG-CSP(1:3)	0.973441	1.146331	1.024337	2.947571	0.338855	1.103135
APG-CSP(1:3)	0.958712	1.206851	1.068932	2.133698	1.277091	0.893998
APG-CSP(1:3)	1.086559	1.295259	1.078068	3.475459	2.01656	0.859529
APG-CSP(1:3)	1.010819	1.272161	1.057487	2.900085	1.208548	0.593887
APG-CSP(1:3)	1.08917	1.315773	1.082389	3.443245	2.117385	0.756312

APG-CSP(1:3)	1.043034	1.304583	1.081454	2.925078	1.893858	0.642389
APG-CSP(1:3)	1.09638	1.359673	1.07246	3.670222	1.893789	0.430575
APG-CSP(3:1)	1.019645	1.367773	1.059276	2.976692	1.236013	-0.00706
APG-CSP(3:1)	1.120779	1.481068	1.036317	4.474826	1.093258	-0.50281
APG-CSP(3:1)	1.124744	1.524248	1.032358	4.578105	0.99451	-0.80197
APG-CSP(3:1)	1.122181	1.525788	1.059937	4.84126	1.895141	-0.42298
APG-CSP(3:1)	1.131429	1.557854	1.118681	3.407533	3.016616	-0.50134
APG-CSP(3:1)	1.238708	1.661483	1.056737	5.539958	1.998848	-1.13355
APG-CSP(3:1)	1.175445	1.606648	1.116401	3.948054	3.134436	-0.66885
APG-CSP(3:1)	1.133266	1.764256	1.097466	6.041556	3.316054	-1.2146

Section 8: ^{1}H NMR Spectra

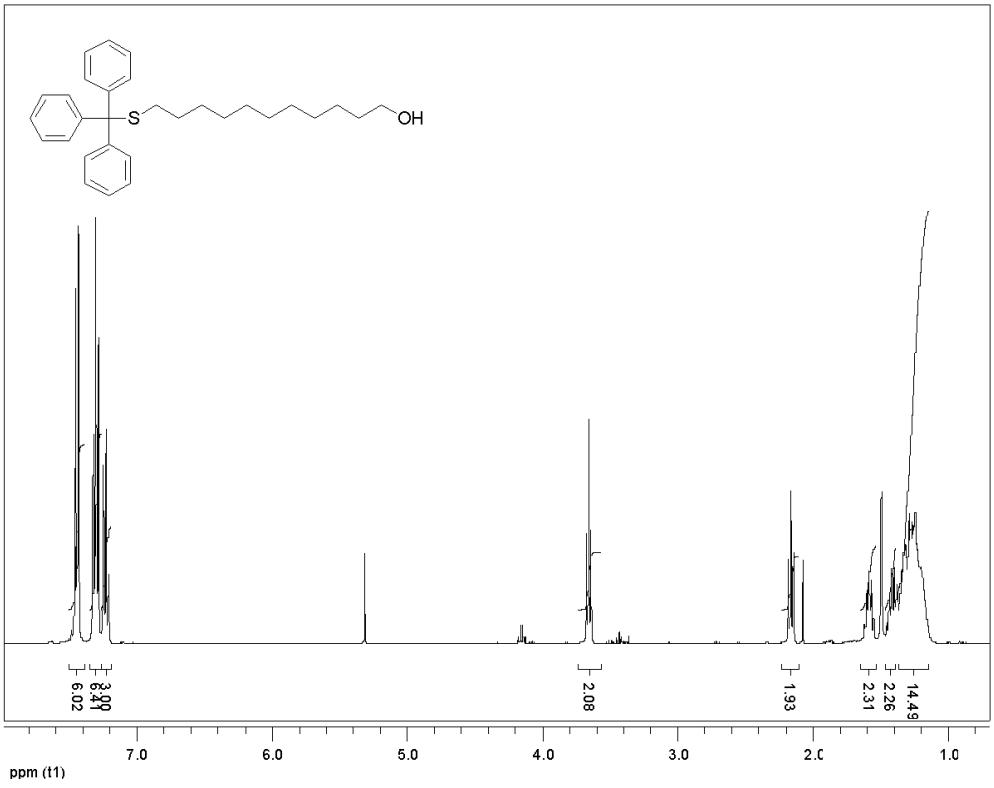

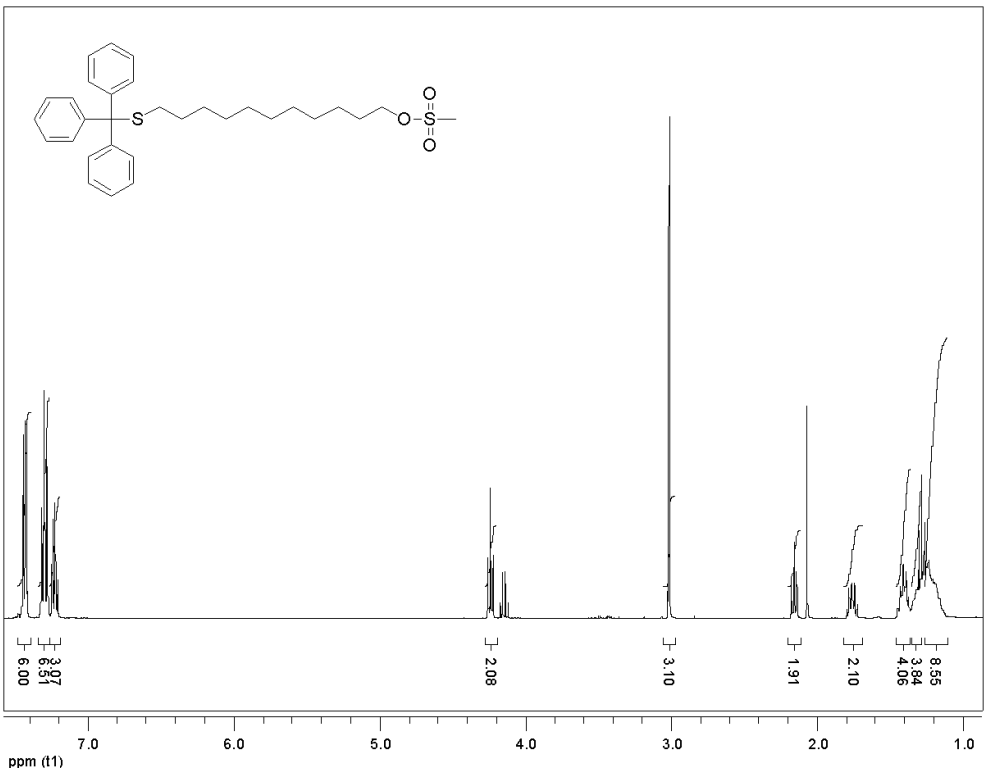
S
O
S
O
O
6.00
6.51
3.07
6.91
2.08
3.10
1.91
2.10
4.06
3.84
8.55
7.0
6.0
5.0
4.0
3.0
2.0
1.0
ppm (t1)

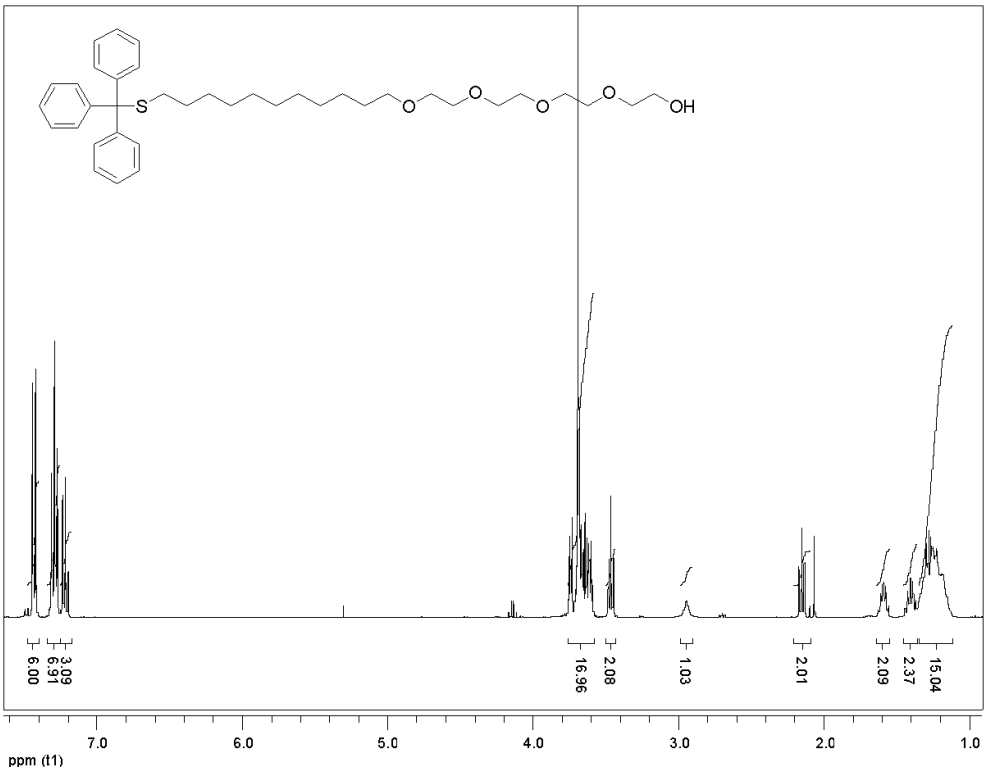
S
O
O
O
O
OH
6.00
6.91
3.09
16.96
2.08
1.03
2.01
2.09
2.37
15.04
7.0
6.0
5.0
4.0
3.0
2.0
1.0
ppm (t1)

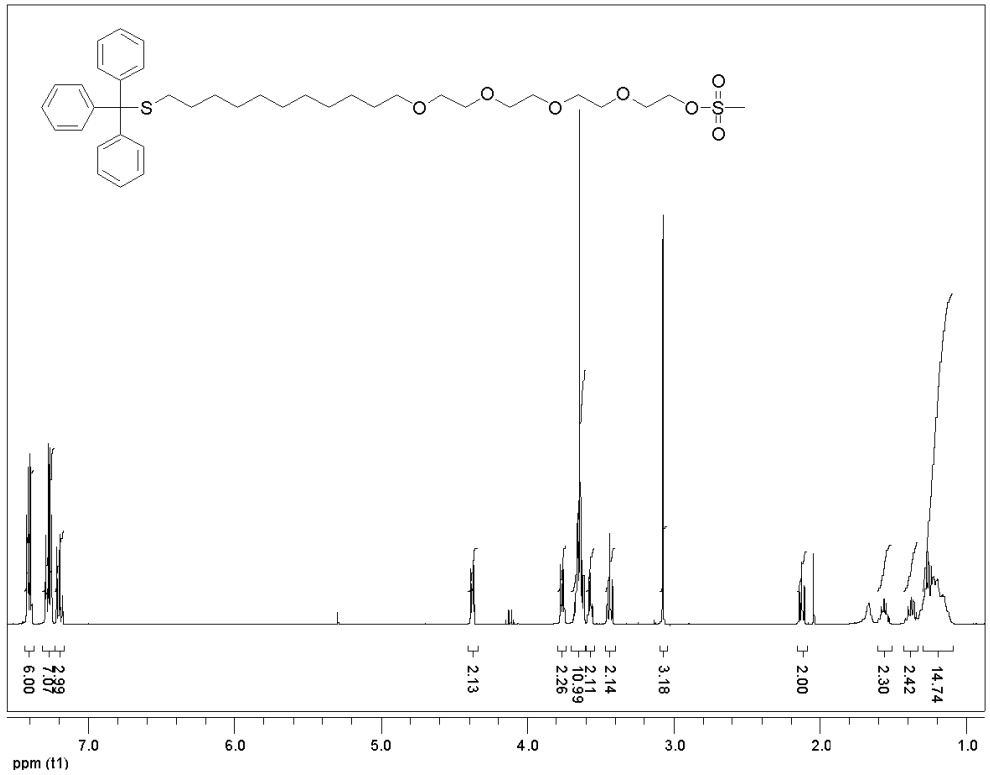
S
O
O
O
O
O
O=S=O
6.00
2.13
10.99
2.11
2.14
3.18
2.00
2.30
2.42
14.74
7.0
6.0
5.0
4.0
3.0
2.0
1.0
ppm (t1)

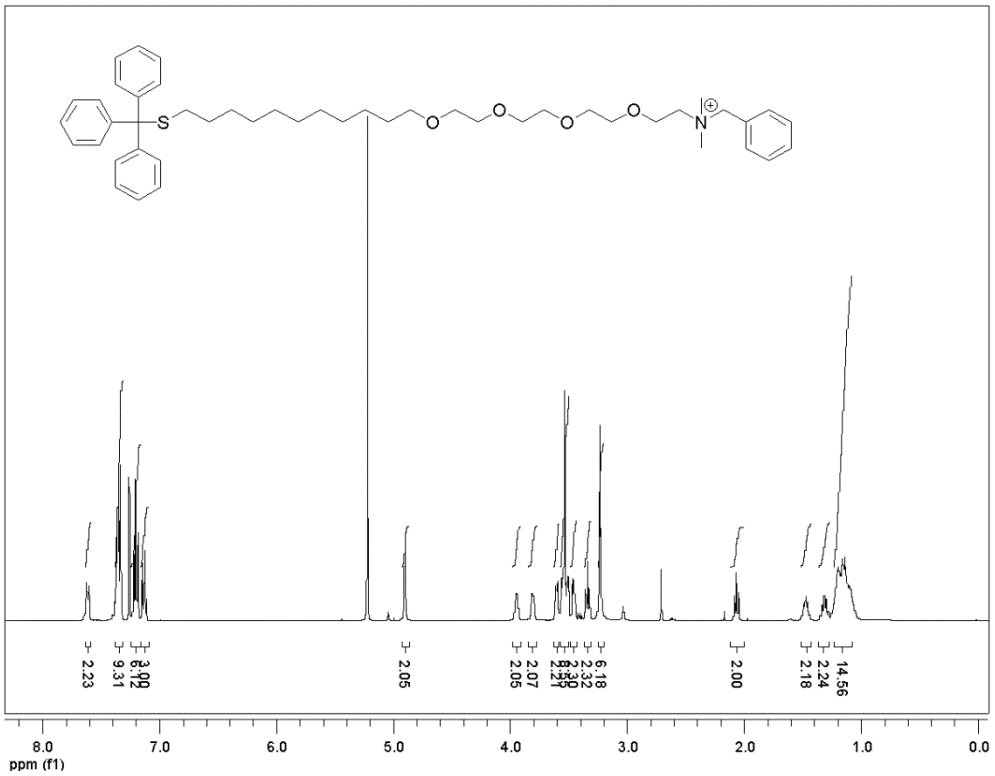
S
O
O
O
O
N
2.23
9.31
2.05
2.05
2.07
6.18
2.00
2.18
2.24
14.56
8.0
7.0
6.0
5.0
4.0
3.0
2.0
1.0
0.0
ppm (f1)

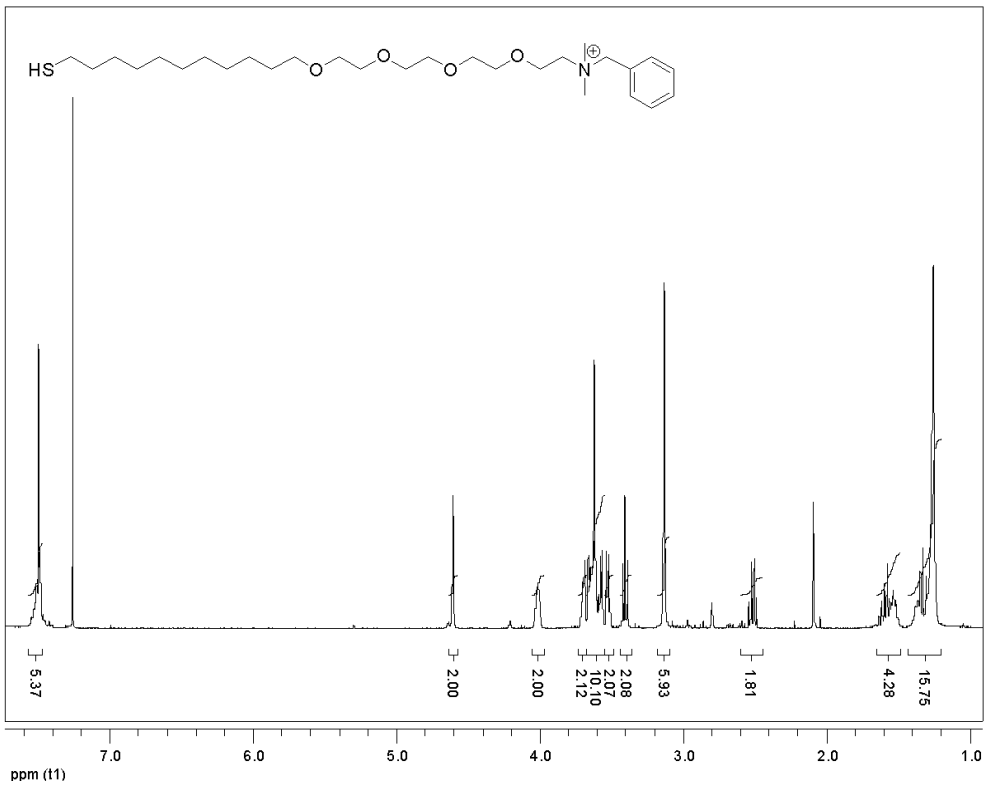
HS
O
O
O
O
N
5.37
2.00
2.00
2.12
10.10
2.07
2.08
5.93
1.81
4.28
15.75
7.0
6.0
5.0
4.0
3.0
2.0
1.0
ppm (t1)

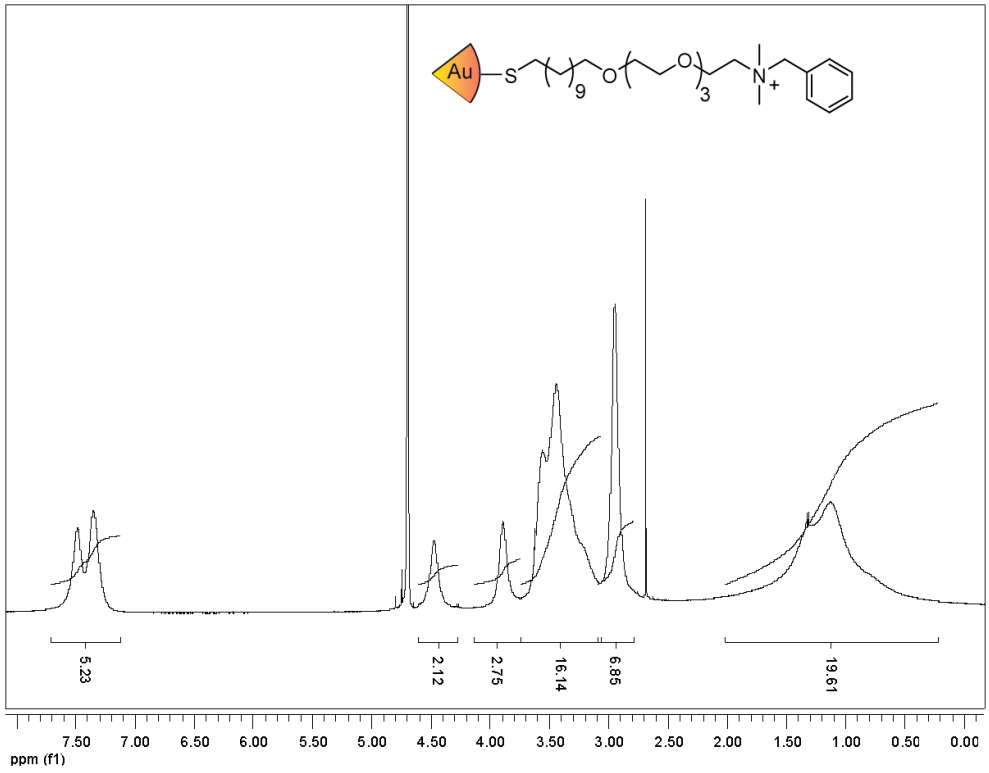
Au
S
9
O
O
3
N+
5.23
2.12
2.75
16.14
6.85
19.61
7.50
7.00
6.50
6.00
5.50
5.00
4.50
4.00
3.50
3.00
2.50
2.00
1.50
1.00
0.50
0.00
ppm (f1)

Supplementary References

1. Ai, H. W. *et al*., Exploration of new chromophore structures leads to the identification of improved blue fluorescent proteins. *Biochemistry* **46**, 5904-5910 (2007).

2. Carroll, P. *et al*, Sensitive detection of gene expression in mycobacteria under replicating and non-replicating conditions using optimized far-red reporters. *PLoS One*. **5**, e9823 (2010).

3. Nandwana, V. *et al*., Patterning of protein/quantum dot hybrid bionanostructures. *J. Inorg. Organomet. Polym. Mater.* **23**, 227-232 (2013).

4. De, M., Rana, S. & Rotello, V. M. Nickel-ion-mediated control of the stoichiometry of His-tagged protein/nanoparticle interactions. *Macromol. Biosci.* **9**, 174-178 (2009).

5. Miranda, A. *et al.*, Enzyme-amplified array sensing of proteins in solution and in biofluids. *J. Am. Chem. Soc.* **132**, 5285-5289 (2010).

6. Bajaj, A. *et al.*, Detection and differentiation of normal, cancerous, and metastatic cells using nanoparticle-polymer sensor arrays. *Proc. Natl. Acad. Sci. U.S.A.* **106**, 10912-10916 (2009).

7. Kanaras, A. G., Kamounah, F. S., Schaumburg, K., Kiely, C. J. & Brust, M. Thioalkylated tetraethylene glycol: a new ligand for water soluble monolayer protected gold clusters. *Chem. Commun.* 2294-2295 (2002).

8. Brust, M., Walker, M., Bethell, D., Schiffrin, D. J. & Whyman, R. Synthesis of thiol-derivatised gold nanoparticles in a two-phase liquid–liquid system. *J. Chem. Soc. Chem. Commun.* 801-802 (1994).

9. Templeton, A. C., Wuelfing, M. P. & Murray, R. W. Monolayer-protected cluster molecules. *Acc. Chem. Res.* **33**, 27-36 (2000).

10. You, C. C., De, M., Han, G. & Rotello, V. M. Tunable Inhibition and Denaturation of Alpha-Chymotrypsin with Amino Acid-Functionalized Gold Nanoparticles. *J. Am. Chem. Soc.* **127**, 12873-12881 (2005).

11. Phillips, R. L. *et al*., Gold Nanoparticle-PPE Constructs as Biomolecular Material Mimics: Understanding the Electrostatic and Hydrophobic Interactions" *Soft Matter* **5**, 607-612 (2009).

12. Dunphy, K. A. *et al*. Oncogenic transformation of mammary epithelial cells by transforming growth factor beta independent of mammary stem cell regulation. *Cancer Cell Int.* **13**, 74 (2013).

13. Nandakumar, D. N., Nagaraj, V. A., Vathsala, P. G., Rangarajan, P. & Padmanaban, G. Curcumin-artemisinin combination therapy for malaria. *Antimicrob. Agents Chemother.* **50**, 1859-1860 (2006).

14. Loewe, S. The problem of synergism and antagonism of combined drugs. *Arzneimittelforschung* **3**, 285-290 (1953).

15. Greco, W. R., Bravo, G. & Parsons, J. C. The search for synergy: a critical review from a response surface perspective. *Pharmacol. Rev.* **47**, 331-385 (1995).

16. R Development Core Team (2010). *R: A language and environment for statistical computing. R Foundation for Statistical Computing*, Vienna, Austria. ISBN 3-900051-07-0, URL http://www.R-project.org.

17. Venables, W. N. & Ripley, B. D. (2002). *Modern Applied Statistics with S*. Fourth Edition. Springer, New York. ISBN 0-387-95457-0.

18. Hardin, J. & Rocke, D. M. The distribution of robust distances. *J. Comput. Graph. Stat.* **14**, 928-946 (2005).